Los Alamos
NATIONAL LABORATORY
research note

Applied Physics Division, X-3
Computational Analysis and Simulation, X-3

To/MS: Distribution
From/MS: S. G. Mashnik, X-3-MCC, MS P365
Phone/FAX: 7-9946/5-4479
Email: mashnik@lanl.gov
Symbol: X-3-RN(U)-07-03, LA-UR-07-xxxx
Date: October 27, 2006

Implementation of CEM03.01 into MCNP6 and its Verification and Validation Running through MCNP6. CEM03.02 Upgrade

Abstract

The latest version of the improved Cascade-Exciton Model (CEM) realized in the event generator CEM03.01 has been updated and extended to describe better Fermi Break-up reactions. Then, it has been incorporated into the transport code MCNP6. Validation and verification study of CEM03.01 running through MCNP6 was performed, including comparison of results by CEM03.01 as a stand-alone code with results by MCNP6 using CEM03.01 and with available experimental data for a large variety of different nuclear reactions. All results obtained with MCNP6 almost coincide with results by CEM03.01 as stand-alone (a very small difference due to different normalizations of the total reaction cross sections used in MCNP6 and in CEM03.01 was observed and is discussed here in details), and agree well with all available experimental data for the tested reactions. After incorporation the updated CEM03.01 into MCNP6 and its verification and validation, the model was improved further to consider the Fermi Break-up mode of reactions during the preequilibrium and evaporation stages of reactions when $A < 13$, that allowed us to avoid production of some unstable residual nuclei that was allowed by previous versions of the model. This physically important feature is not considered yet by any other reaction simulation models available today in the world. We call the latest version of our model considering this important feature as CEM03.02. This work was performed by S. G. Mashnik (X-3-MCC) in collaboration with R. E. Prael (X-3-MCC) with important contribution and support from K. K. Gudima of the Academy of Science of Moldova and in consultation with and a permanent support from A. J. Sierk (T-16).

1. Introduction

MCNP5 1.4.0 [1] is the most advanced transport code available today to the public from RSICC to describe interactions of neutrons, photons, and electrons with thick and thin targets. However, it uses only nuclear data libraries and does not employ any high-energy event generators, therefore it can not be used for Proton Radiography (PRAD) as a radiographic probe

for the Advanced Hydro-test Facility applications. This is why the US Department of Energy has supported during several past years development of the MCNP6 transport code [2], an extension of MCNP5 to higher energies and to consider transport of protons and many other elementary particles as well as of light- and heavy-ions, and has supported our work on the development of improved versions of the Cascade-Exciton Model (CEM) of nuclear reactions and the Los Alamos version of the Quark-Gluon String Model (LAQGSM) as event generators for MCNP6 able to describe reactions induced by particles and nuclei at energies up to about 1 TeV/nucleon [3]-[6].

The latest versions of our event generators, CEM03.01 and LAQGSM03.01, [3]-[6] have significantly improved Intra-Nuclear Cascade (INC) models, updated preequilibrium, evaporation, fission, Fermi Break-up, and coalescence models able to describe better than their predecessors emission of complex particles and light fragments, and were extended to describe photonuclear reactions up to tens of GeV. On the whole, CEM03.01 and LAQGSM03.01 describe nuclear reactions much better than their predecessors and other similar codes available to the nuclear physics community. They have been benchmarked on a variety of particle-particle, particle-nucleus, and nucleus-nucleus reactions at energies from 10 MeV to 800 GeV per nucleon, and have been or are being incorporated as event generators into the transport codes MCNP6, MCNPX, and MARS.

However, both CEM03.01 and LAQGSM03.01 had until recently some problems in a correct description of some light unstable fragments produced from some nuclear reactions on light- and medium-mass targets. This problem was addressed and solved in the work described here.

This Research Note presents a summary and progress report on a further development of CEM03.01 to address the problem of production of some unstable light isotopes from some nuclear reactions, on incorporation of the updated and improved this way CEM03.01 into MCNP6, on its verification and validation running through MCNP6, and on the latest improvement of CEM03.01 already incorporated into MCNP6 to consider the Fermi Break-up mode of reactions during the preequilibrium and evaporation stages of reactions, that resulted in the upgrade of our event generator we refer here to as CEM03.02.

2. Improvement of CEM03.01 before its incorporation into MCNP6

CEM03.01 is available to the public as the RSICC Code Package PSR-532 starting from March 2006. This version of the code was implemented into a working version of MCNPX (alpha version of MCNPX 2.6.B [7]) and we were notify later on by Gregg McKinney about several bugs he or other users of that version of MCNPX did found in CEM03.01. In very rear cases, for some reactions on light targets, those bugs led to events where some complex particles created as "residual nuclei" after the preequilibrium or evaporation stages of reactions were "lost", and as a result, a "non-conservation" of the baryon number for the whole reaction would occur. In other very rare cases, "dineutrons" or "neutron stars", i.e., residual nuclei that consisted of only two or more neutrons (without any protons) could appear in some very rare events of some reactions as simulated by the Fermi Break-up model used in CEM03.01. Those bugs were related with the

FORTRAN implementation of parts of several preequilibrium, evaporation, and Fermi Break-up routines and some historical old small errors in those routines but not with the wrong physics of the nuclear reaction models considered by CEM03.01.

All the mentioned above bugs were fixed before we implemented CEM03.01 into MCNP6. In addition, Dick Prael did a special investigation of the Fermi Break-up model used by CEM03.01. The routines that describe the Fermi Break-up model were written some twenty years ago in the group of Prof. Barashenkov at JINR, Dubna, Russia, and are far from being perfect, though they are used currently without any changes in many transport codes like GEANT4, SHIELD, CASCADE, SONET, CASCADO, etc. First, these routines allow in rare cases production of some light unstable fragments like ^{5}He, ^{5}Li, ^{8}Be, ^{9}B, etc., as a result of a break-up of some light excited nuclei. Second, these routines allowed in some very rare cases even production of "neutron stars" (or "proton stars"), i.e., residual "nuclei" produced via Fermi Break-up that consist of only neutrons (or only protons). Last, as was discovered by Dick Prael, in some very rare cases, these routines could even crash the code, due to cases of 0/0. All these problems of the Fermi Break-up model routines were addressed and solved by Dick Prael. For instance:

1) In the routine fermid.f, multiple passes through the break-up loop to permit the decay of intermediate resonance states that may be products of a decay have been added. At the present time, only ^{5}He, ^{8}Be, and ^{9}B fall in this category. Illustrations of how other such states may be allowed have been added.

2) In the routine razval.f, the logic to allow all possible break-up channels to be accessed has been corrected. When coupled with the change in the routine wechan.f, this allows the break-up of ^{8}C to ^{4}He + 4p by a five-body break-up.

3) In wechan.f, the Coulomb barriers were made slightly penetrable, allowing decay by Coulomb-blocked channels if no other possibilities exist.

4) A small change that will allow a "proton star" to break-up even at low excitation energy was made; i.e. Mass(n protons) = n*Mass(1 proton).

All the mentioned above improvements of the Fermi Break-up routines were made before CEM03.01 was incorporated into MCNP6. The improved code was verified, validated, and tested against dozens of experimentally measured nuclear reactions on different light targets. Several examples of such results, namely excitation functions for the production of ^{12}N, ^{11}C, ^{10}C, ^{10}Be, ^{7}Be, ^{9}Li, ^{8}Li ^{6}He, ^{4}He, ^{3}He, t, d, p, and n from p+^{12}C are presented in Figs. 1 and 2 together with experimental data and results by the "standard CEM03.01", i.e., with the bugs mentioned in the beginning of this Section fixed but without the improvement of the Fermi Break-up model, and with calculations by the old CEM95 [8] code published in Ref. [9]. One can see that the version of CEM03.01 with the improved Fermi Break-up model describes, generally, reactions better than the "standard" version without such improvements. This is in addition to solving the problems of the production of some unstable fragments like ^{5}He, ^{8}Be, ^{9}B, of possible "proton starts", and to possible crash the code due to very rare cases of 0/0.

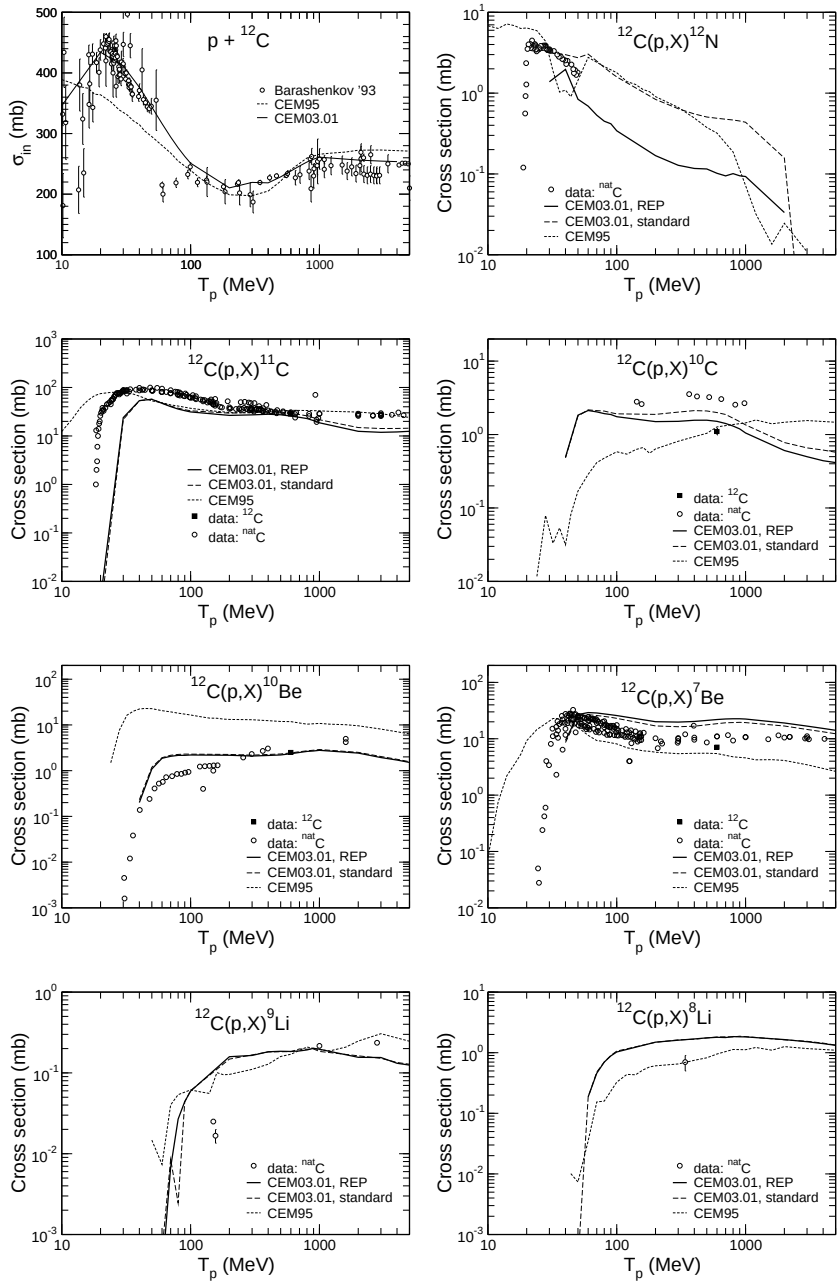

Figure 1: Total inelastic cross section and excitation functions for the production of ^{12}N, ^{11}C, ^{10}C, ^{10}Be, ^{7}Be, ^{9}Li, and ^{8}Li from p+^{12}C calculated with the old CEM95 code in Ref. [9], with the recent version of CEM, CEM03.01, available from RSICC [3] but with several observed bugs fixed as described above (labeled as "CEM03.01, standard"), and with its last updated version considering the Fermi Break-up model as improved recently by R. E. Prael (labeled as "CEM03.01, REP") as described above. The experimental data are from Refs. [10-15]; see details on experimental data in [9].

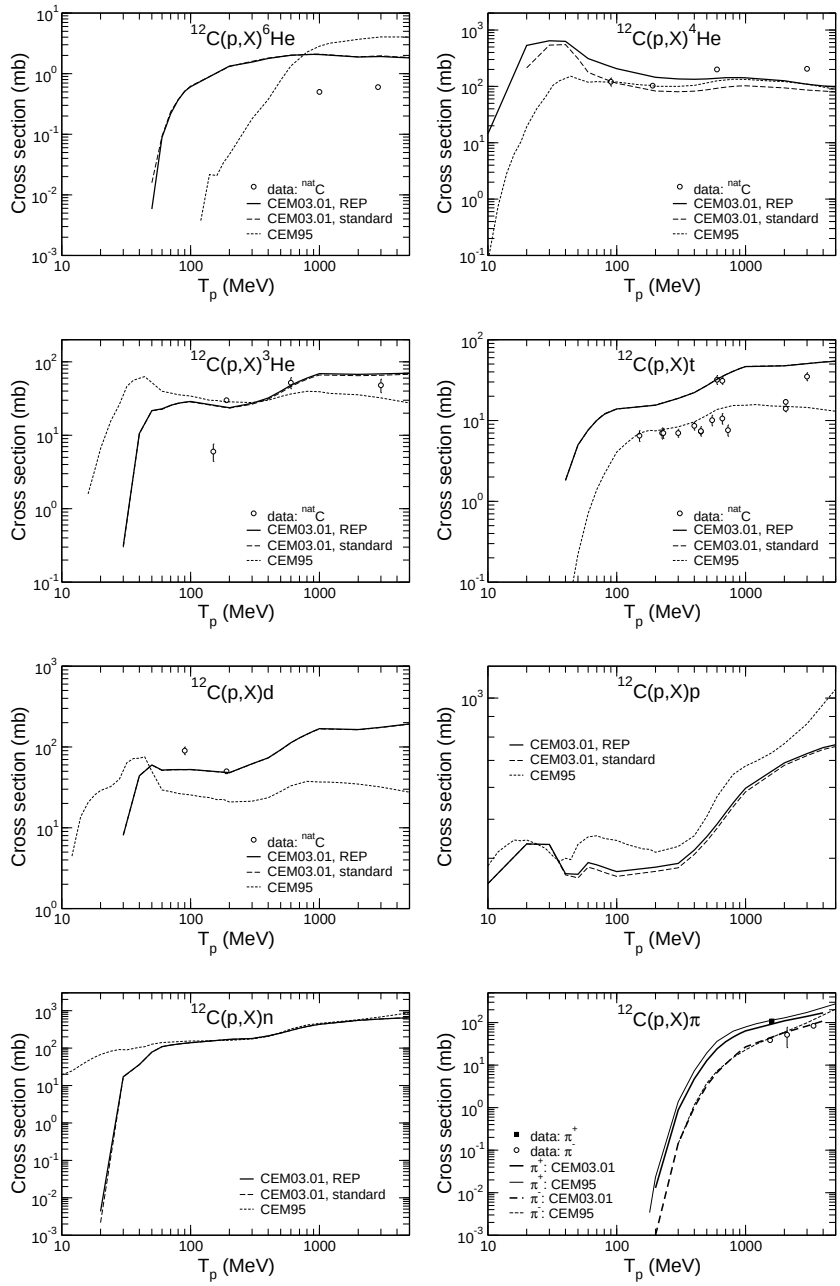

Figure 2: Excitation functions for the production of ^{6}He, ^{4}He, ^{3}He, t, d, p, n, π^+, π^0, and π^- from p+^{12}C calculated with the old CEM95 code in Ref. [9], with the recent version of CEM, CEM03.01, available from RSICC [3] but with several observed bugs fixed as described above (labeled as "CEM03.01, standard"), and with its last updated version considering the Fermi Break-up model as improved recently by R. E. Prael (labeled as "CEM03.01, REP") as described above. The experimental data are from Refs. [12,16,17].

3. Implementation of the updated CEM03.01 into MCNP6 and its verification and validation running through MCNP6

The updated and improved as described above CEM03.01 was incorporated into MCNP6 (Artifact artf4394 in SourceForge). Regression test problems # 78, 79, 80, 81, and 82 were added to MCNP6 to reflect this implementation and to test CEM03.01 running through MCNP6 and to compare the results with predictions by CEM03.01 as a stand-alone code and with available experimental data for different characteristics of the following nuclear reactions:

#78: 4 GeV p + ^{12}C;

#79: 800 MeV p + ^{197}Au;

#80: 5 GeV p + ^{27}Al;

#81: 1.5 GeV π^+ + ^{56}Fe;

#82: 730 MeV p + ^{27}Al.

The reactions included in these regression test problems were chosen not at random but after a careful analysis of the available experimental data and of possible problems with results by CEM03.01 for some reactions. So, problems #78 and 80 were chosen because of experimental data for different excitation functions available for these reactions around these energies, and because one may expect production (with a very little probability) of some unstable final isotopes by CEM03.01, that would be an unphysical result that should be fixed. Problem #82 was chosen because of rich experimental data on spectra (both double-differential and angle- and energy-integrated) of protons, π^+, and π^- measured at many angles in Ref. [19] from interaction of 730 MeV protons with Pb, Cu, Al, C, and H (see Figs. 3 and 4). The input of this test problem can be used after only little modifications to calculate other types of spectra extensively measured lately in the literature because of their relevance to some current ADC applications, namely spectra of neutrons from reactions induced by protons (see Fig. 5 with experimental data from Ref. [20]). Problem #81 examples another type of nuclear reactions measured recently [21]: Spectra of neutrons produced from pion-induced reactions (see Fig. 6). Finally, problem #79 corresponds to one of the measured recently at GSI reactions using the inverse kinematics technique, namely 800 MeV/nucleon ^{197}Au + p [22]. These measurements provide a very rich set of cross sections (see Fig. 7) for the production of practically all possible isotopes from such reactions in a "pure" form, *i.e.*, individual cross sections from a specific given bombarding isotope (or target isotope, when considering reactions in the usual kinematics, p + A). Such cross sections are much easier to compare to models than the "camouflaged" data from γ-spectrometry measurements.

To be able to compare results by CEM03.01 as a stand-alone code with results by MCNP6 using CEM03.01 event generator, we use the GENXS option in MCNP6 that provides capabilities to generate double-differential particle production cross sections and residual nuclei production cross sections from high-energy nuclear interaction models implemented into MCNP6 in a cross

section generation mode, without particle transport [18]. The option is invoked by specifying **genxs inxcNN** on the **tropt** card of the MCNP6 input file **inpNN** (**NN** identifies here the number of the regression MCNP6 test problems; see examples of **inp** and **inxc** files for the test problems #78-82 on the following pages). The content and the format of the edited output of MCNP6 is determined from the auxiliary input files **inxcNN** that define the energy (momentum) and angle bin boundaries of the spectra of the chosen types of particles to be included in the output and other details. Ref. [18] provides a comprehensive description of the **tropt** card and of the format of the **inxcNN** files, therefore we do not repeat this here but only show the **inp** and **inxc** files for the regression test problems #78-82 on the following pages.

Results by CEM03.01 as a stand-alone code are compared with results by MCNP6 using CEM03.01 obtained according to these MCNP6 regression test problems and with available experimental data in Figs. 3-7.

Fig. 3 presents spectra of protons at 30, 60, 90, 120, and 150 deg from 730 MeV p + Pb, Cu, Al, and C calculated by MCNP6 using CEM03.01 (dashed histograms) and by CEM03.01 as a stand-alone code (solid histograms) compared with available experimental data [19] (symbols). The MCNP6 input files for the results presented in Fig. 3 are very similar to the one of the regression test problem #82: The only difference is that with **inp82** we simulate only 10,000 inelastic events, *i.e.*.

```
nps 10000
```

while the statistics of the Monte Carlo simulations showed in Fig. 3 is of one million inelastic events, *i.e.*.

```
nps 1000000
```

and the mass and charge numbers in the MCNP6 input card

```
m1   13027 1.0
```

and in the title cards of both **inp82** and **inxc82** files should be changed for nuclei-targets different of Al, respectively. One can see that results by MCNP6 using CEM03.01 agree very well with results by CEM03.01 as a stand-alone code and with experimental data. However, we see that practically all proton spectra calculated by MCNP6 are a little higher than the results by CEM03.01 as a stand-alone code (the difference is of an order of only a few percents or less). Let us postpone the discussion of the reason of this small difference for the conclusion of this Section.

inp78:

```
GENXS Test: p+C12 at 4 GeV
  1  1  1.0   -1 2 -3
  2  0        -4 (1:-2:3)
  3  0         4

c ---------------------------------------------------------------
  1  cz  4.0
  2  pz  -1.0
  3  pz  1.0
  4  so  50.0

c ---------------------------------------------------------------
  m1   6012 1.0
  sdef erg = 4000 par = 5 dir = 1 pos = 0 0 0 vec 0 0 1
  imp:h 1 1 0
  phys:h 4000
  mode   h
  tropt genxs inxc78  nreact on  nescat off
c ---------------------------------------------------------------
  print 40 110 95
  nps 10000
  prdmp 2j -1
```

inxc78:

```
Test problem 64: p+C12 at 4 GeV
2 1 1 /
Test problem 64: Angular edit
0 -180 9 /
/
1 5 6 7 8 21 22 23 24 /
Test problem 64: Energy edit
71 0 9 /
-0.1 10000 /
1 5 6 7 8 21 22 23 24 /
```

inp79:

```
Comparison Test: p+Au197 at 800 MeV
  1  1  1.0   -1 2 -3
  2  0        -4 (1:-2:3)
  3  0         4

c ---------------------------------------------------------------
  1  cz  4.0
  2  pz  -1.0
  3  pz  1.0
  4  so  50.0

c ---------------------------------------------------------------
  m1   79197 1.0
  sdef erg = 800 par = 5 dir = 1 pos = 0 0 0 vec 0 0 1
  imp:h 1 1 0
  phys:h 1000
  mode   h
  tropt genxs inxc79  nreact on  nescat off
c ---------------------------------------------------------------
  print 40 110 95
  nps 5000
  prdmp 2j -1
```

inxc79:

```
Comparison Test: p+Au197 at 800 MeV
1 1 1 /
Cross Section Edit
56 0 9 /
5. 10. 15. 20. 25. 30. 35. 40. 45. 50. 55. 60. 65. 70. 75. 80.
85. 90. 95. 100. 120. /
1 5 6 7 8 21 22 23 24 /
```

inp80:

```
Comparison Test: p+Al27 at 5 GeV
  1  1  1.0   -1 2 -3
  2  0        -4 (1:-2:3)
  3  0         4

c ---------------------------------------------------------------
  1  cz  4.0
  2  pz  -1.0
  3  pz  1.0
  4  so  50.0

c ---------------------------------------------------------------
  m1   13027 1.0
  sdef erg = 5000 par = 5 dir = 1 pos = 0 0 0 vec 0 0 1
  imp:h 1 1 0
  idum 66
  phys:h 5000
  mode   h
  tropt genxs inxc80  nreact on  nescat off
c ---------------------------------------------------------------
  print 40 110 95
  nps 10000
  prdmp 2j -1
```

inxc80:

```
Comparison Test: p+Al27 at 5 GeV
1 1 1 /
Cross Section Edit
56 0 9 /
5. 10. 15. 20. 25. 30. 35. 40. 45. 50. 55. 60. 65. 70. 75. 80.
85. 90. 95. 100. 120. /
1 5 6 7 8 21 22 23 24 /
```

inp81:

```
Comparison Test: pip+Fe56 at 1.5 GeV
  1  1  1.0   -1 2 -3
  2  0        -4 (1:-2:3)
  3  0         4

c ---------------------------------------------------------------
  1  cz  4.0
  2  pz  -1.0
  3  pz  1.0
  4  so  50.0

c ---------------------------------------------------------------
  m1   26056 1.0
  sdef erg = 1500 par = 6 dir = 1 pos = 0 0 0 vec 0 0 1
  imp:+ 1 1 0
  phys:+ 2000
  mode   +
  tropt genxs inxc81  nreact on  nescat off
c ---------------------------------------------------------------
  print 40 110 95
  nps 10000
  prdmp 2j -1
```

inxc81:

```
Comparison Test: pip+Fe56 at 1.5 GeV
1 1 1 /
Cross Section Edit
34 -7 9 /
1 2 3 4 5 6 7 8 9 10 20 30 40 50 60 70 80 90 100 200 300
400 500 600 700 800 900 1000 1100 1200 1300 1400 1500 1600 /
155. 145. 95. 85. 35. 25. 0. /
1 5 6 7 8 21 22 23 24 /
```

inp82:

```
Comparison Test: p+Al27 at 730 MeV
  1  1  1.0   -1 2 -3
  2  0        -4 (1:-2:3)
  3  0         4

c ---------------------------------------------------------------
  1  cz  4.0
  2  pz  -1.0
  3  pz  1.0
  4  so  50.0

c ---------------------------------------------------------------
  m1   13027 1.0
  sdef erg = 730 par = 5 dir = 1 pos = 0 0 0 vec 0 0 1
  imp:h 1 1 0
  phys:h 1000
  mode   h
  tropt genxs inxc82  nreact on  nescat off
c ---------------------------------------------------------------
  print 40 110 95
  nps 10000
  prdmp 2j -1
```

inxc82:

```
Comparison Test: p+Al27 at 730 MeV
1 1 1 /
Cross Section Edit
52 -11 9 /
5. 10. 15. 20. 25. 30. 35. 40. 45. 50. 55. 60. 65. 70. 75. 80.
85. 90. 95. 100. 120. /
155. 145. 125. 115. 95. 85. 65. 55. 35. 25. 0. /
1 5 6 7 8 21 22 23 24 /
```

Fig. 4 shows examples of π^- and π^+ angle-integrated energy spectra from the same reactions as shown in Fig. 3, and calculated with the same inputs of MCNP6 and CEM03.01. Just as we saw above for the proton spectra, the pion spectra from these reactions calculated by MCNP6 using CEM03.01 agree very well with results by CEM03.01 as a stand-alone code and with experimental data, and again the results by MCNP6 are a little higher than the results by CEM03.01 as a stand-alone code (the difference is again of an order of only a few percents or less).

Fig. 5 shows examples of double differential neutron spectra at 15, 30, 60, 90, 120, and 150 deg from 1.5 GeV and 800 MeV p + Pb calculated by MCNP6 using CEM03.01 (dashed histograms) and by CEM03.01 as a stand-alone code (solid histograms) compared with recent measurements by Ishibashi *et. al.* [20] (symbols). The **inp** and **inxc** MCNP6 files for these reactions are very similar to the ones of the regression test problem #82 used to obtain results shown in Figs. 3 and 4: The only small differences are in the energy and angle bin boundaries in the MCNP6 file **inxc**, and in the value of the energy of the bombarding protons in the MCNP6 file **inp**, and, of course, in the title cards of both **inp** and **inxc** files. For both reactions shown in Fig. 5 we have simulated one million inelastic events. The agreement between results by MCNP6 using CEM03.01 and by CEM03.01 as a stand-alone code with experimental data is very similar to what we had above for proton and pion spectra: Neutron spectra calculated by MCNP6 using CEM03.01 agree very well with results by CEM03.01 as a stand-alone code and with experimental data [20], and again the results by MCNP6 are a little higher than the results by CEM03.01 as a stand-alone code (the difference is again of an order of only a few percents or less).

Fig. 6 shows examples of double differential neutron spectra at 30, 90, and 150 deg but from other type of nuclear reactions, namely, from interactions of 1.5 GeV π^+ with ^{56}Fe. The MCNP6 input files for the results presented in Fig. 6 are very similar to the one of the regression test problem #81: The only difference is that with **inp81** we simulate only 10,000 inelastic events, while the statistics of the Monte Carlo simulations showed in Fig. 6 is of one million inelastic events, respectively. One can see that results by MCNP6 using CEM03.01 agree very well with results by CEM03.01 as a stand-alone code and with experimental data. Just as for other reactions discussed above, we see again that the neutron spectra calculated by MCNP6 are a little higher than the results by CEM03.01 as a stand-alone code (the difference is again of an order of only a few percents or less).

Finally, Fig. 7 shows mass and charge distributions of the product yields from the reaction 800 MeV/A ^{197}Au+p and of the mean kinetic energy of these products, and the mass distributions of the cross sections for the production of thirteen elements with the charge Z from 20 to 80 measured recently at GSI [22] compared with results by MCNP6 using CEM03.01 and with predictions by CEM03.01 as a stand-alone code.

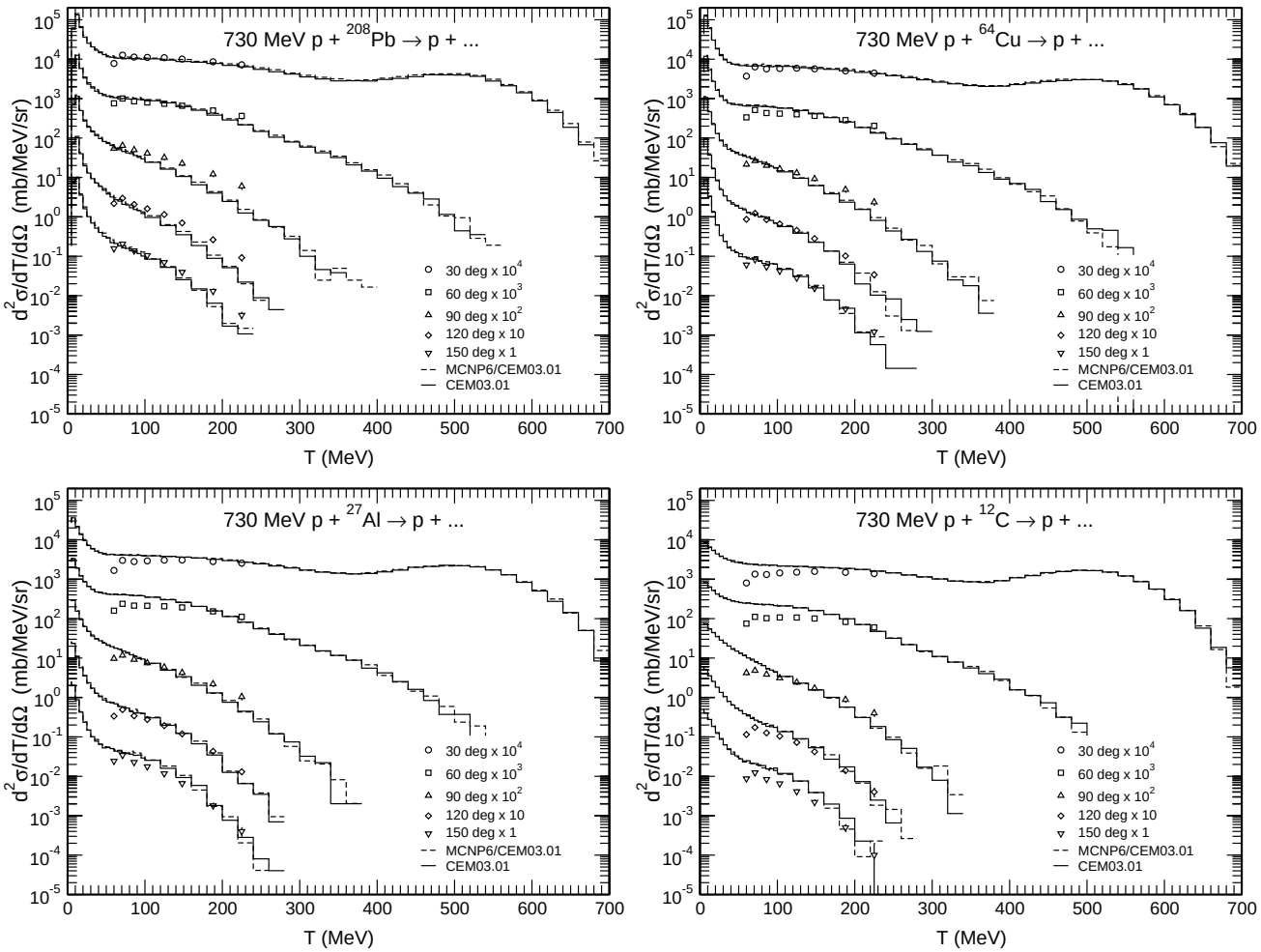

Figure 3: Experimental [19] double differential proton spectra at 30, 60, 90, 120, and 150 deg from 730 MeV p + Pb, Cu, Al, and C (symbols) compared with results by MCNP6 using CEM03.01 (dashed histograms) and by CEM03.01 as a stand-alone code (solid histograms).

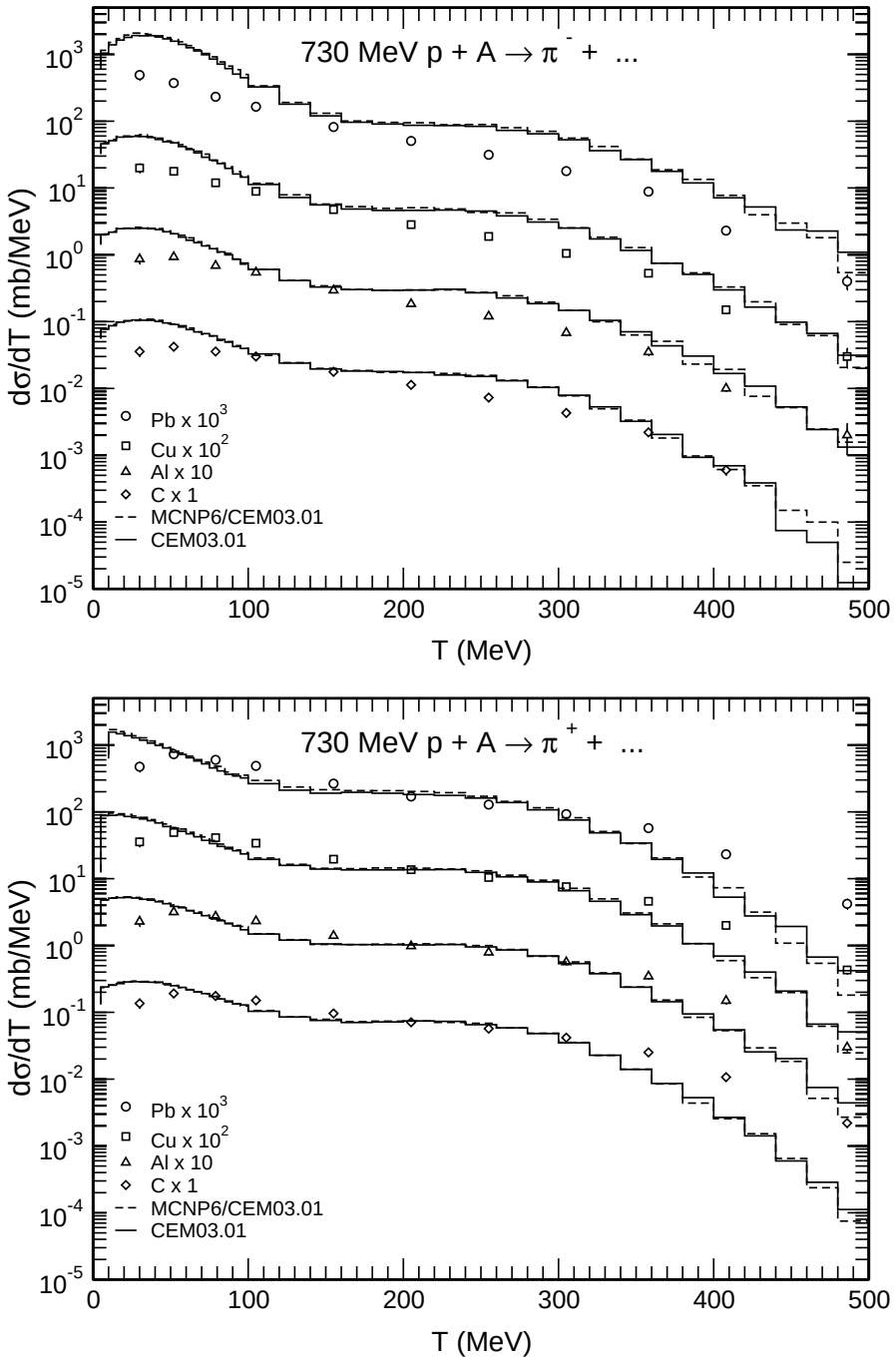

Figure 4: Experimental [19] angle-integrated energy spectra of negative and positive pions from 730 MeV p + Pb, Cu, Al, and C (symbols) compared with results by MCNP6 using CEM03.01 (dashed histograms) and by CEM03.01 as a stand-alone code (solid histograms).

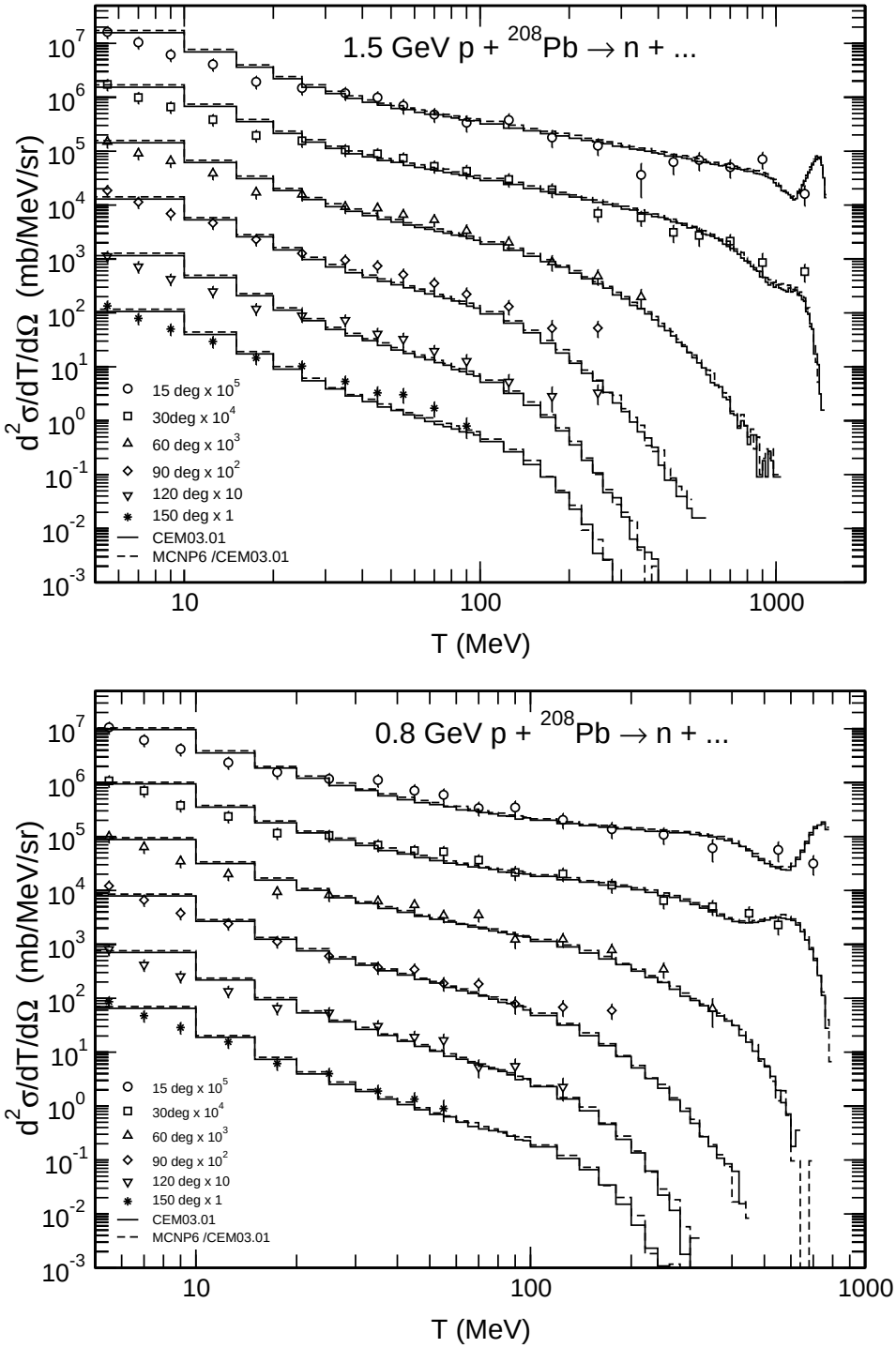

Figure 5: Experimental [20] double differential neutron spectra at 15, 30, 60, 90, 120, and 150 deg from 1.5 GeV and 800 MeV p + Pb (symbols) compared with results by MCNP6 using CEM03.01 (dashed histograms) and by CEM03.01 as a stand-alone code (solid histograms).

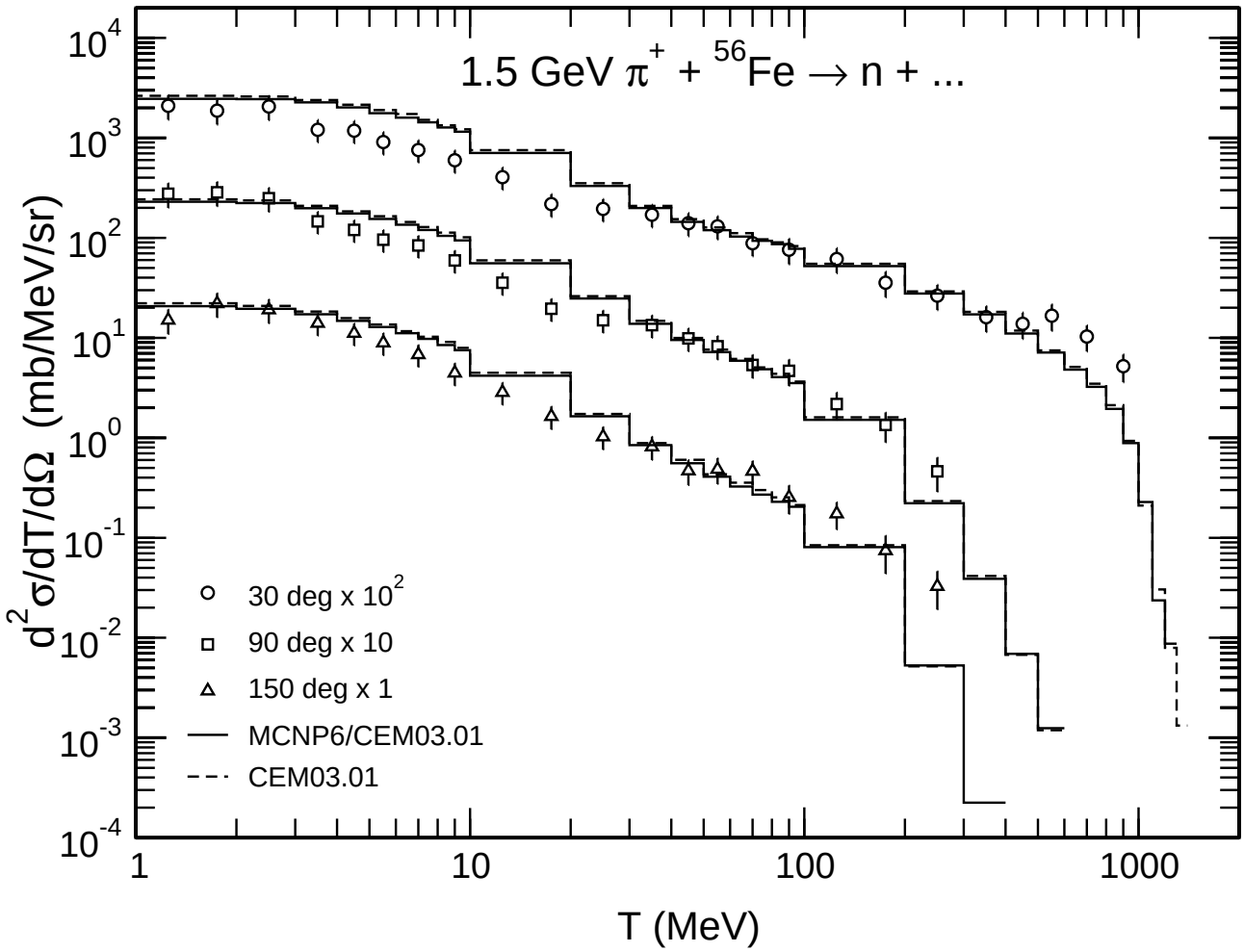

Figure 6: Experimental [21] double differential neutron spectra at 30, 90, and 150 deg from 1.5 GeV $\pi^+ + {}^{56}$Fe (symbols) compared with results by MCNP6 using CEM03.01 (solid histograms) and by CEM03.01 as a stand-alone code (dashed histograms).

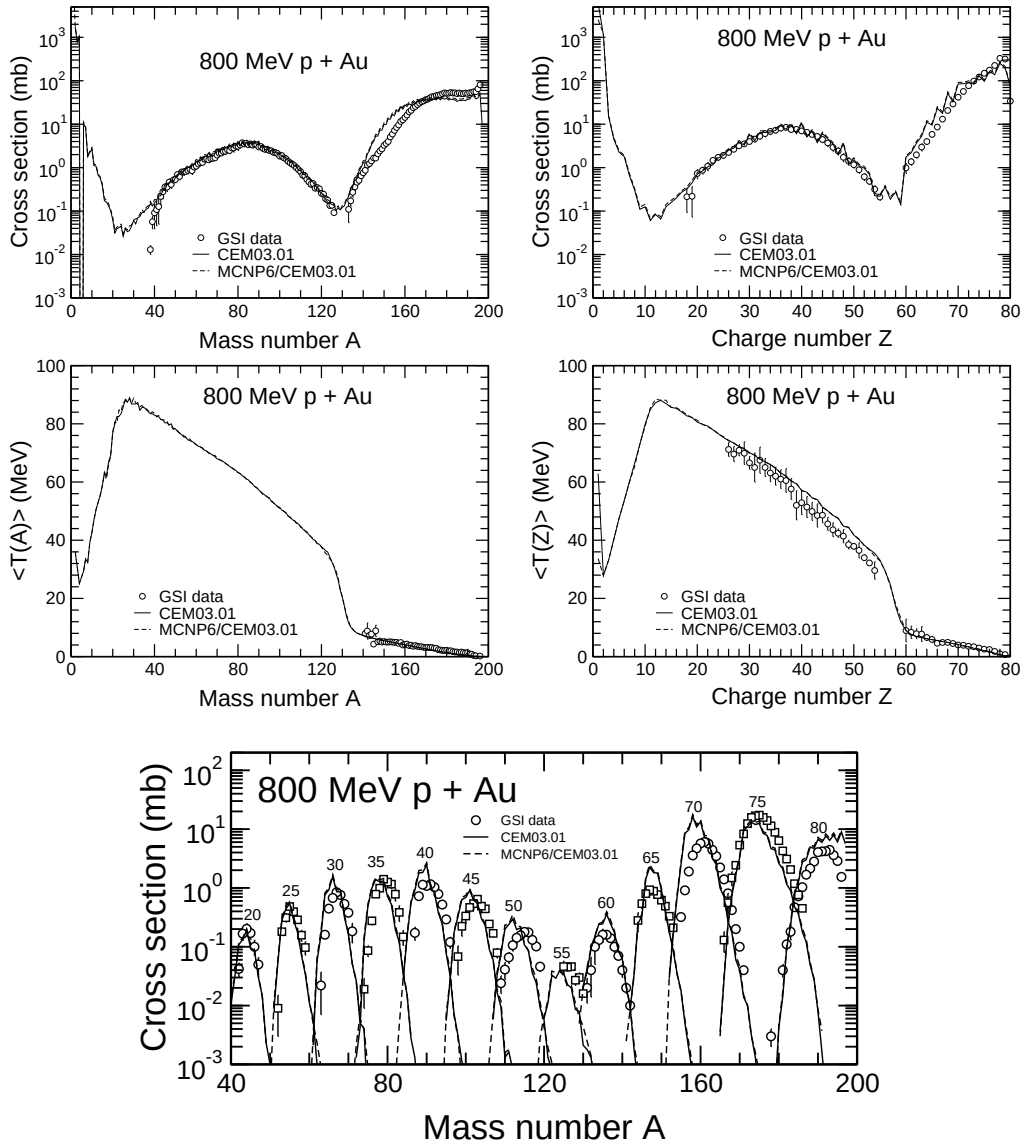

Figure 7: The measured [22] mass and charge distributions of the product yields from the reaction 800 MeV/A ^{197}Au+p and of the mean kinetic energy of these products, and the mass distributions of the cross sections for the production of thirteen elements with the charge Z from 20 to 80 (open symbols) compared with CEM03.01 as a stand-alone code results (solid lines) obtained using the input shown in Example 7 of Appendix 1 (the corresponding output is shown in Example 7 of Appendix 2) of the CEM03.01 User Manual [3] and with results by MCNP6 using CEM03.01 (dashed lines) as provided by the MCNP6 regression test problem #79. The results shown in this figure are for ten million simulated inelastic events (**limc=10000000** in the input of CEM03.01, that corresponds to the card **nps 10000000** in the MCNP6 input) and the option **nevtype=66** in the input of CEM03.01, that corresponds to the use of the card **idum 66** in the MCNP6 input.

The MCNP6 results shown in Fig. 7 correspond to the regression test problem #79. The results shown in this figure are for ten million simulated inelastic events (**limc=10000000** in the input of CEM03.01, that corresponds to the card **nps 10000000** in the MCNP6 input) and the option **nevtype=66** in the input of CEM03.01, that corresponds to the use of the card **idum 66** in the MCNP6 input after the card

```
imp:h 1 1 0
```

of the MCNP6 file **inp79**. The option **nevtype=66** in the input of CEM03.01 that corresponds to the use of the card **idum 66** in the MCNP6 input file allows to evaporate up to 66 types of nucleons, complex particles, and light fragments from excited compound nuclei (see details in [3]).

Just as we had for proton, neutron, and pion spectra from the reactions discussed above, we see that results by MCNP6 using CEM03.01 for the GSI measured characteristics shown in Fig. 7 agree very well with results by CEM03.01 as a stand-alone code and with the GSI data [22]. We see again that the results by MCNP6 are a little higher than the results by CEM03.01 as a stand-alone code, and the difference is again of an order of only a few percents or less.

To summarize, for all the reactions shown in Figs. 3 to 7 we obtained similar results: Results by MCNP6 using CEM03.01 agree very well with results by CEM03.01 as a stand-alone code and with available experimental data, but the results by MCNP6 are a little higher than the results by CEM03.01 as a stand-alone code; the difference is of an order of only a few percents or less. One may understand this difference easily if to recall that MCNP6 and CEM03.01 as a stand-alone code use different normalizations for the total reaction cross sections: Following MARS, MCNP6 uses for all reactions and incident energies discussed here the approximations by Barashenkov and Polanski [27] for the total inelastic cross sections to normalize the results. On the other hand, CEM03.01 uses the NASA systematics by Tripathi, Cucinota, and Wilson [24] to normalize results from neutron- and proton-induced reactions, and calculates itself using the Monte Carlo method the total reaction cross section for reactions induced by pions, like the one shown in Fig. 6 (see details in [3]).

To understand better the little difference in the absolute normalization of results by MCNP6 and results by CEM03.01 as a stand-alone code observed here, we have compile from the literature the experimental data on total reaction (absorption) cross sections proton (and n, d, t, ^{3}He, and ^{4}He) interactions with the target-nuclei discussed above, C, Al, and Au; we did not find enough experimental data for Cu and Pb discussed above, therefore we include in our study the neighbor nuclei of Fe and Bi, respectively. Figs. 8 to 12 show our compilation of experimental data on total reaction cross sections for these targets together with different approximations for them available in the literature, namely, the Dostrovsky *et. al.* [23] approximation, the NASA systematics by Tripathi, Cucinota, and Wilson [24] used by CEM03.01, a parameterization by Kalbach [25], an approximation by Tang, Srinivasan, and Azziz [26], and results calculated with the phenomenological code CROSEC by Barashenkov and Polanski [27] used by MCNP6.

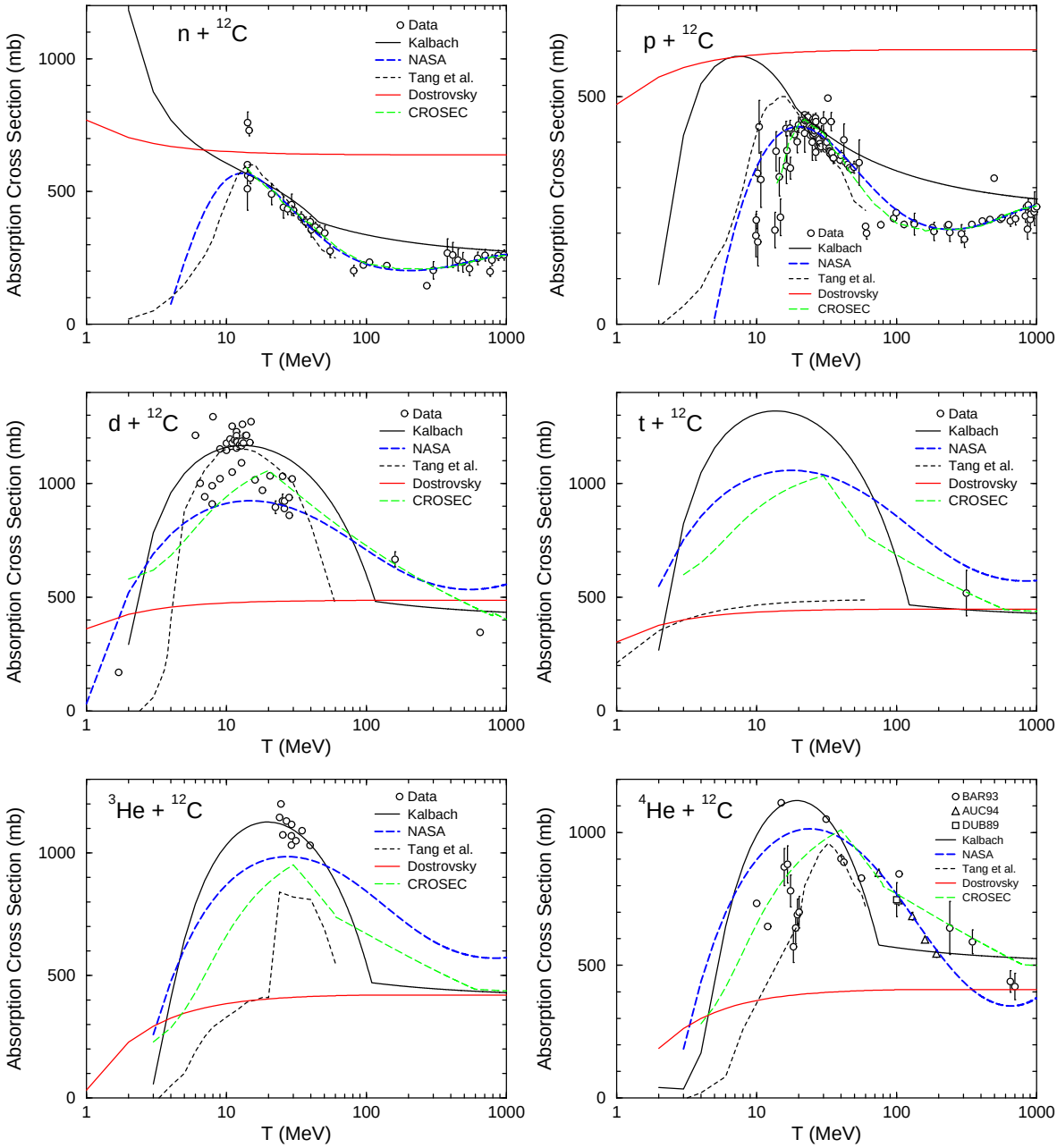

Figure 8: Comparison of experimental data on total reaction (absorption) cross sections for n, p, d, t, ^{3}He, and ^{4}He on ^{12}C with the Dostrovsky *et. al.* [23 approximation, the NASA systematics by Tripathi, Cucinota, and Wilson [24], a parameterization by Kalbach [25], an approximation by Tang, Srinivasan, and Azziz [26], and results calculated with the phenomenological code CROSEC by Barashenkov and Polanski [27]. Most of the data points (circles, either without a special label or labeled as "BAR93") shown here are from the compilation by Barashenkov [10]; several data points are by Auce *et al.* [28] (triangles labeled as "AUC94"), and a data point for ^{4}He is measured by Dubar *et al.* [29] (the square labeled as "DUB89").

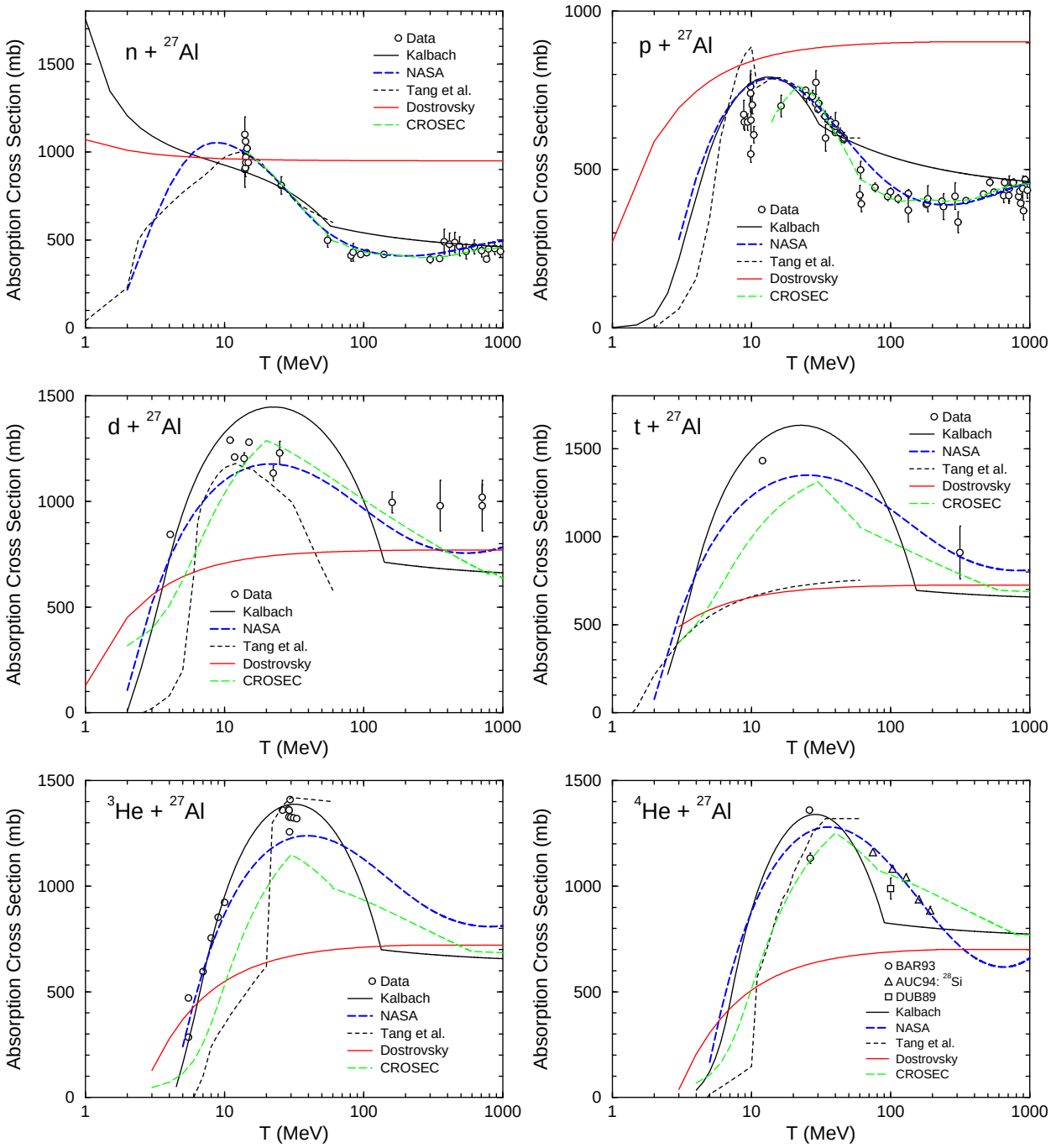

Figure 9: The same as in Fig. 8 but for the nucleus-target ^{27}Al.

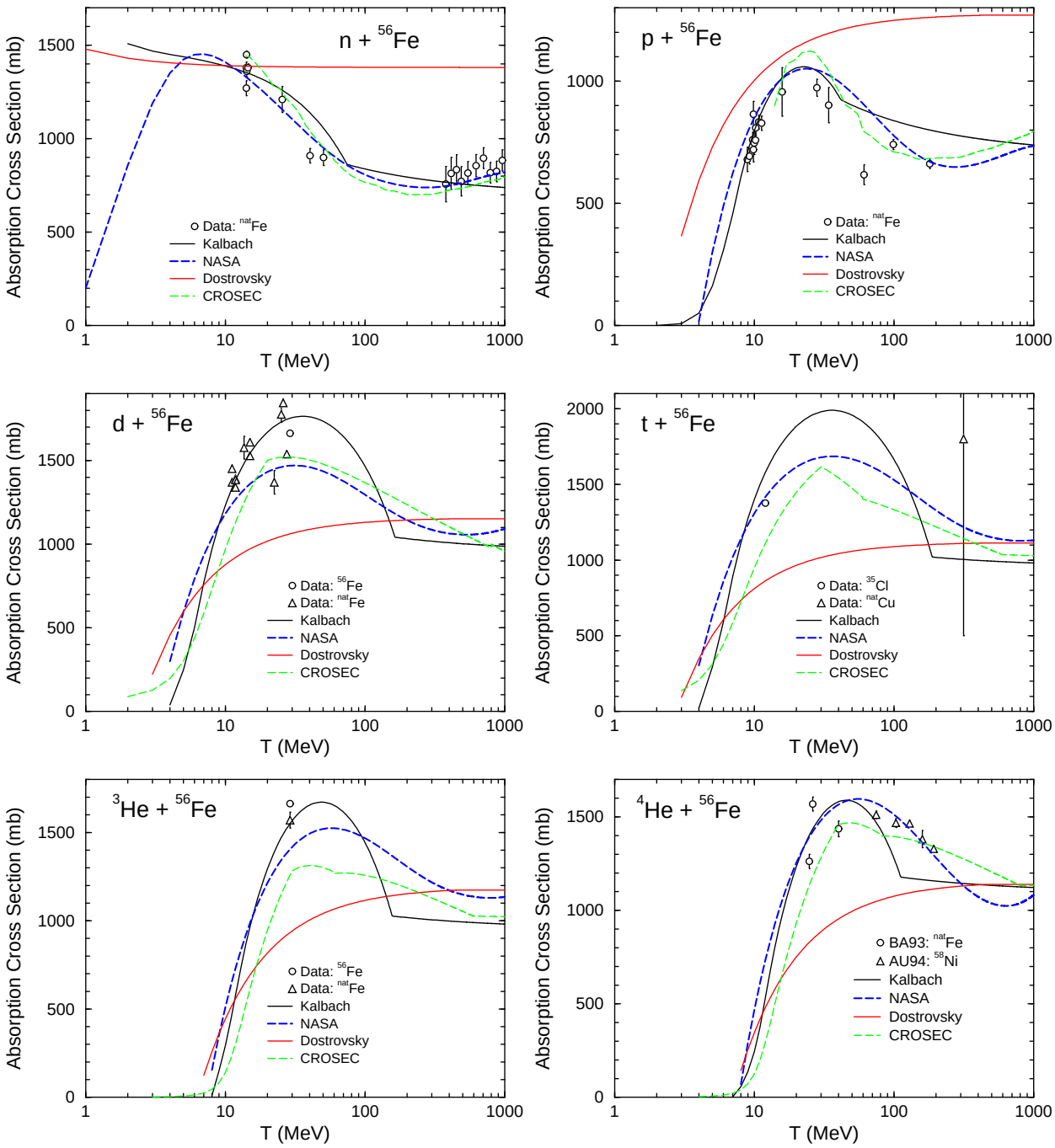

Figure 10: The same as in Fig. 8 but for the nucleus-target ^{56}Fe.

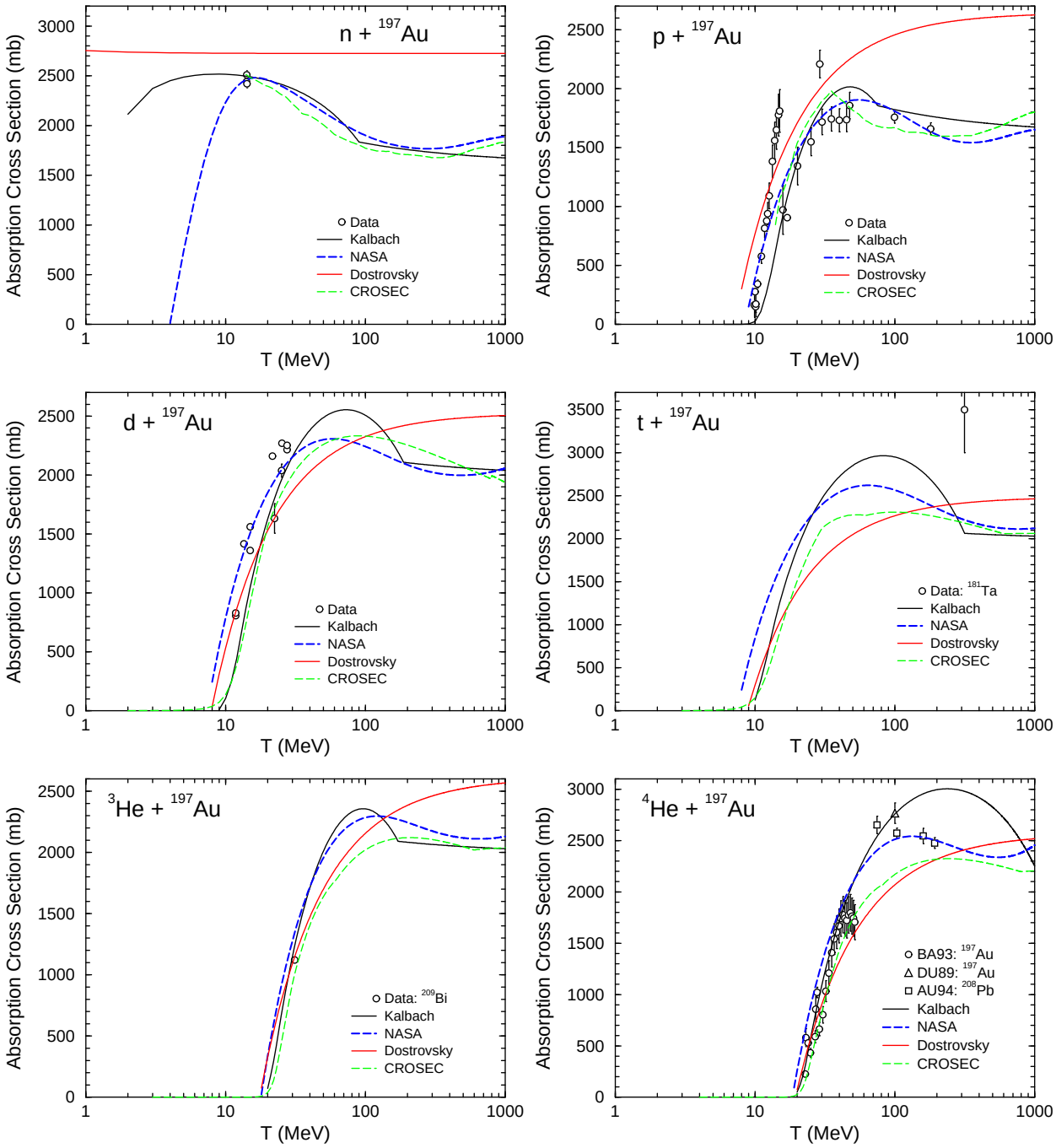

Figure 11: The same as in Fig. 8 but for the nucleus-target ^{197}Au.

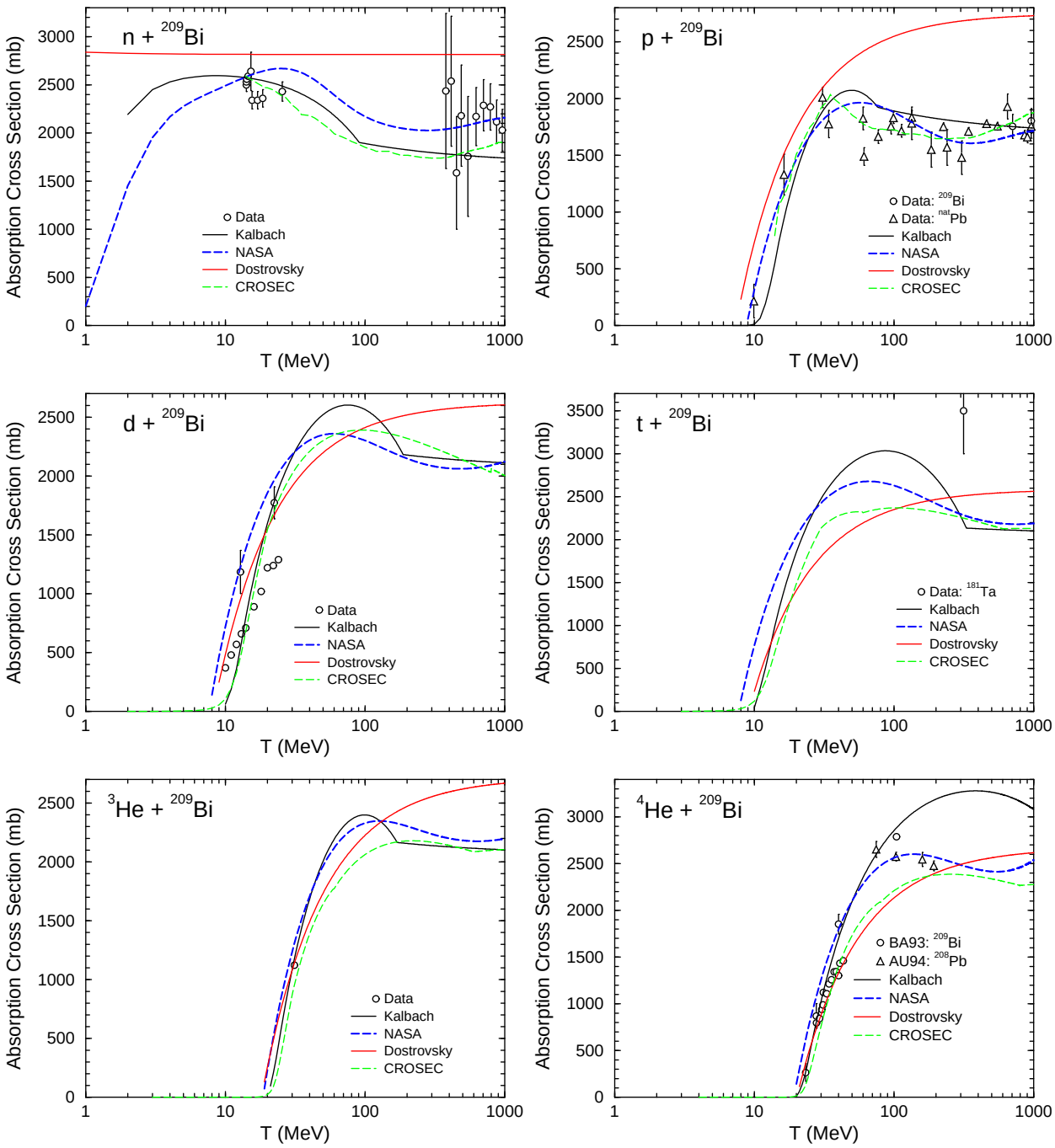

Figure 12: The same as in Fig. 8 but for the nucleus-target ^{209}Bi.

We have obtained results very similar to the ones shown in Figs. 8 to 12 for dozens of other nuclei-targets, but we do not show them here as we do not discuss here those nuclei. As one can see from Figs. 8 to 12, the NASA systematics by Tripathi, Cucinota, and Wilson [24] used by CEM03.01 and the approximations of Barashenkov and Polanski [27] used by MCNP6 describe the total reaction cross sections induced by protons better than other approximations discussed here do, and agree well with each other. However, the approximations by Barashenkov and Polanski [27] used by MCNP6 for all reactions and incident energies discussed above and shown in Figs. 3 to 7 are a little higher than the NASA systematics by Tripathi, Cucinota, and Wilson [24] used by CEM03.01, and the difference is of an order of only a few percents or less. This explains completely the little difference we got above between results by MCNP6 using CEM03.01 and by CEM03.01 as a stand-alone code.

From Figs. 8 to 12, we may observe that the NASA systematics by Tripathi, Cucinota, and Wilson [24] agree a little better than the approximations of Barashenkov and Polanski [27] with available experimental data for total reaction cross sections for reactions induced not only by protons, but also by n, d, t, ^{3}He, and ^{4}He transported by MCNP6. In addition, the NASA systematics [24] are smoother than the approximations of Barashenkov and Polanski [27], that looks to us as physically grounded better.

This is why we suggest to consider in the future a possible permanent replacement in MCNP6 of the approximations by Barashenkov and Polanski [27] used at present with the NASA systematics by Tripathi, Cucinota, and Wilson [24], as an improved feature of MCNP6.

4. CEM03.02 Upgrade

After incorporation the updated CEM03.01 into MCNP6 and its verification and validation as described above, the model was improved further to consider the Fermi Break-up mode of reactions during the preequilibrium and evaporation stages of reactions when $A < 13$, that allowed us to avoid production of some unstable residual nuclei that was allowed by previous versions of the model.

This further improvement of CEM03.01 was necessary because a few results from the MCNP6 regression test problems #80, 81, and 82 as provided by the updated version of CEM03.01 incorporated into MCNP6 (Artifact artf4394 in SourceForge) were wrong: With that version, we got a little yield of some unstable products, like ^{4}H in problem #82, ^{4}Li in problem #81, and $^{4-8}$H, ^{13,14}He, ^{4}Li, and ^{6,8}Be in problem #80. The summed yield of all these unstable products is less than 0.1% from the total yield of all products, so that production of these unstable nuclides affects less than 0.1% the other correct and good results from these test problems. But these unstable nuclides are unphysical and CEM03.01 should be fixed to get rid of such unphysical results.

Such a fix was done via a "Complex Bug Fix" (Artifact artf4617 in SourceForge) by replacing the description of reactions at the preequilibrium and/or evaporation stages of reactions done originally in CEM03.01 (and in LAQGSM03.01) by the Modified Exciton Model (MEM) and/or

Generalized Evaporation Model (GEM) for any excited nuclei (see details in [3, 5]) with a description of such reactions with the Fermi Break-up model, in cases when the mass numbers of excited nuclei are $A < 13$. Such improvements was done in CEM03.01 incorporated into MCNP6 (artf4617) as well as in CEM03.01 as a stand-alone code kept in the independent "CEM event generator" project of SourceForge and in the preequilibrium and evaporation parts of our high-energy event generator LAQGSM03.01 kept in the independent "LAQGSM" project of SourceForge. To the best of our knowledge, this physically important feature is not considered yet by any other reaction simulation models available today in the world. We call the latest version of our event generators considering this important feature as CEM03.02 and LAQGSM03.02, respectively; these versions of our event generators do not produce any more unphysical unstable products.

Examples of several results by CEM03.02 compared with results by previous version, CEM03.01, and by older versions CEM95 and CEM2k and with experimental data for a number of relevant reactions are presented Figs. 13 to 17. Fig. 13 presents the mass distribution of the product yields from the reaction 730 MeV p + ^{27}Al calculated with CEM03.01 without considering the Fermi Break-up mode during the preequilibrium and evaporation stages of reactions and with the extended here version of the code referred here to as CEM03.02 that does consider the Fermi Break-up mode during the preequilibrium and evaporation stages of reactions. One can see that CEM03.01 does provide a little yield of unphysical unstable ^{5}He (just like do the older versions of our event generators CEM95 and CEM2k and as do similar models of other authors available in the literature), while the last version, CEM03.02 does not produce any more such unstable unphysical nuclides. The results by CEM03.02 also agree a little better with available experimental data (red squares on Fig. 13) than results by CEM03.01. Similar results were obtained also for several other reactions on other light targets.

Our results show that CEM03.02 does not predict unstable unphysical nuclides and describes the yields of most products a little better that CEM03.01 or older versions of CEM. The question about how the spectra of different particles from different nuclear reactions are described by CEM03.02 in comparison with older versions of the code is not obvious. We studied this question on several reactions and Fig. 14 presents examples of particle spectra calculated with CEM03.01 and CEM03.02 for the reaction 730 MeV p + Al. We see that spectra of n, p, d, t, ^{3}He, and ^{4}He calculated by CEM03.02 that uses the Fermi Break-up model to describe disintegration of exited nuclei with $A < 13$ are almost the same as such spectra calculated by CEM03.01 that uses the preequilibrium and evaporation models to describe such reactions when $A > 12$ after the INC stage of reactions. This result is very interesting from a physical point of view, it is not trivial at all and could not be forecast easily in advance. We see that spectra of different particles predicted by different models are almost the same. In other words, the theoretical spectra of particles do not depend much on the models we use to calculate them, but depend mostly on the final phase spaces calculated by these models: If the phase spaces calculated by different models are correct and near to each other, than the spectra of secondary

particles calculated by these models would be also near to each other and would be not very sensitive to the dynamics of reactions considered (or not) by the models we use.

Fig. 15 shows examples of experimental neutron spectra at 15, 30, 60, 90, 120, and 150 deg from 3.0, 1.5, 0.8, and 0.597 GeV p + Al (symbols) compared with results by CEM03.01 without considering the Fermi Break-up mode during the preequilibrium and evaporation stages of reactions (dashed histograms), with CEM03.02 that does consider the Fermi Break-up mode during the preequilibrium and evaporation stages of reactions (solid histograms), and with the old version of the code, CEM95 [8]. We see that the results by CEM03.02 and CEM03.01 agree much better with the data at neutron energies of 20-100 MeV (where the contribution from the preequilibrium mode is the most important) than the results by the old CEM95 do. Results by CEM03.02 for these neutron spectra almost coincide with results by CEM03.01, just as observed above for spectra of n, p, d, t, ^{3}He, and ^{4}He shown in Fig. 14.

From Figs. 16 and 17, we see that, as a rule, CEM03.02 describes a little better than CEM03.01 (and significantly, by several orders of magnitudes, better than the older codes CEM95 and CEM2k) many excitation functions for the production of different isotopes from proton-induced reactions on Al and Si, in addition to the fact that CEM03.02 does not predict production of unphysical unstable nuclides while previous versions do so. Similar results were obtained for other reactions on light targets. However, some excitation functions calculated by CEM03.02 agree with available experimental data a little worse than those calculated by CEM03.01. We believe that the agreement of results by CEM03.02 with experimental data can be improved by fitting carefully the parameter r_0 in Eq. (74) of Ref. [3] against large sets of different experimental data relevant to Fermi Break-up. This agreement could be probably also improved by improving the description of the Coulomb barriers in the Fermi Break-up model (see details in Section 2.6 of Ref. [3]). Such a study would require a lot of calculations and routine work for hundreds of different nuclear reactions induced by different projectiles on light and medium targets; it is outside the aim of the present work and could be performed in the future as an independent work on improving our event generators.

5. Summary

The latest version of the improved Cascade-Exciton Model (CEM) realized in the event generator CEM03.01 has been updated and extended to describe better Fermi Break-up reactions. After that, it has been incorporated into the transport code MCNP6. Validation and verification study of CEM03.01 running through MCNP6 was performed, including extensive comparisons of results by CEM03.01 as a stand-alone code with results by MCNP6 using CEM03.01 and with available experimental data for a large variety of different nuclear reactions. All results obtained with MCNP6 almost coincide with results by CEM03.01 as stand-alone and agree very well with all available experimental data for the tested reactions. However, we observed a very small difference due to different normalizations of the total reaction cross sections used in MCNP6 and in CEM03.01.

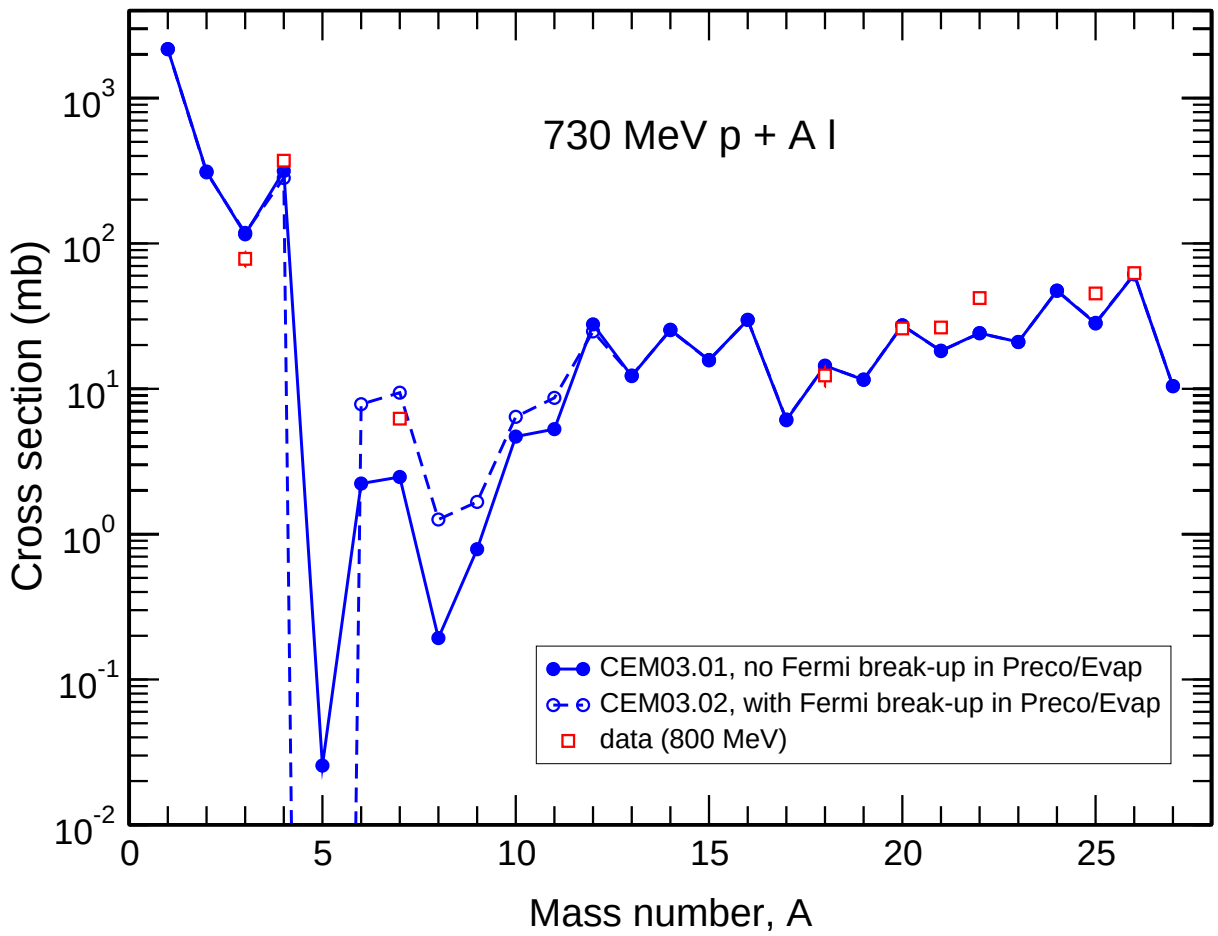

Figure 13: Mass distribution of the product yields from the reaction 730 MeV p + ^{27}Al calculated with CEM03.01 without considering the Fermi Break-up mode during the preequilibrium and evaporation stages of reactions (solid circles connected with a solid line) and with the extended here version of the code referred here and below to as CEM03.02 that does consider the Fermi Break-up mode during the preequilibrium and evaporation stages of reactions (open circles connected with a dashed line) compared with experimental data available at a nearby energy of 800 MeV from the T-16 Lib compilation [30] (open red squares).

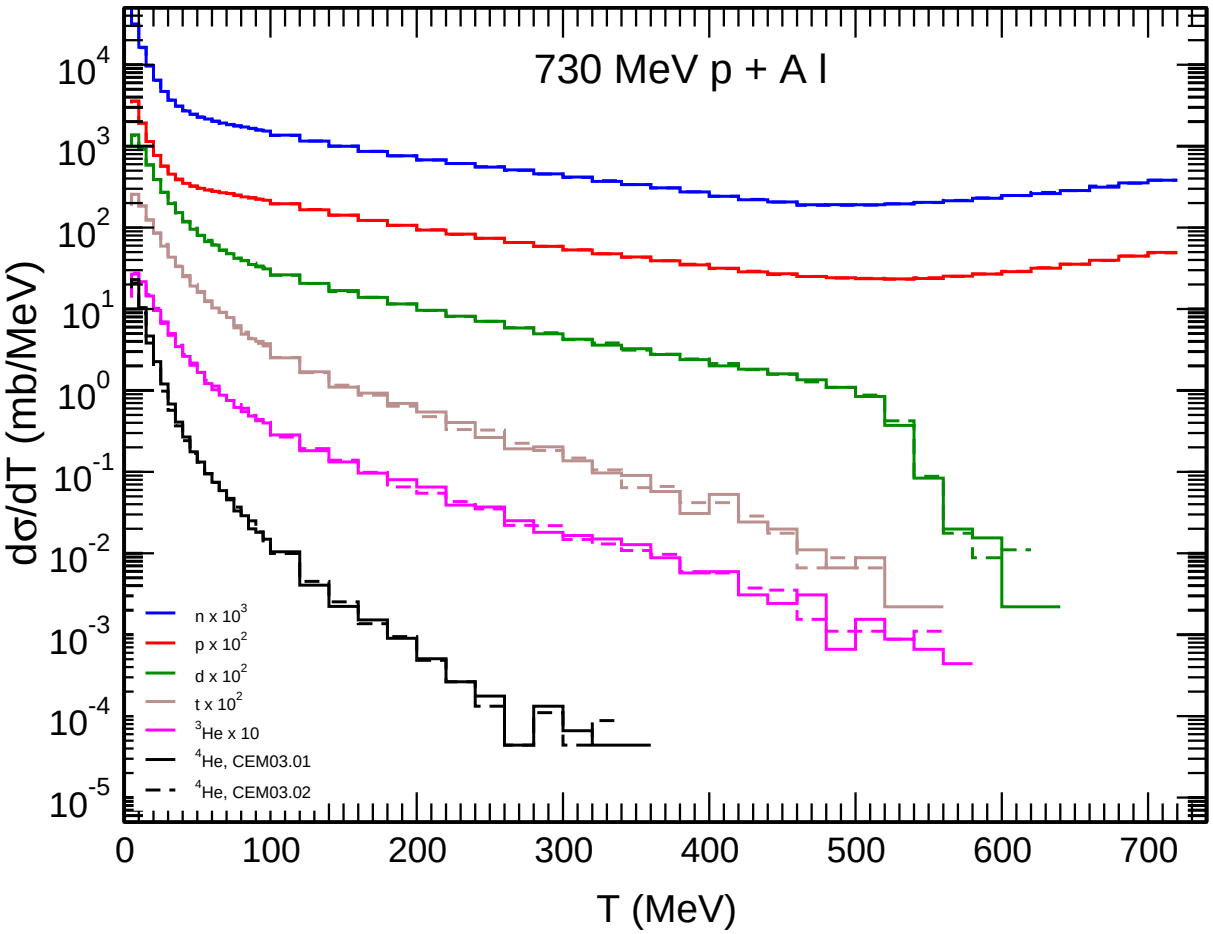

Figure 14: Angle-integrated energy spectra of secondary n, p, d, t, ^{3}He, and ^{4}He from the reaction 730 MeV p + ^{27}Al calculated with CEM03.01 without considering the Fermi Break-up mode during the preequilibrium and evaporation stages of reactions (solid histograms) and with CEM03.02 that does consider the Fermi Break-up mode during the preequilibrium and evaporation stages of reactions (dashed histograms).

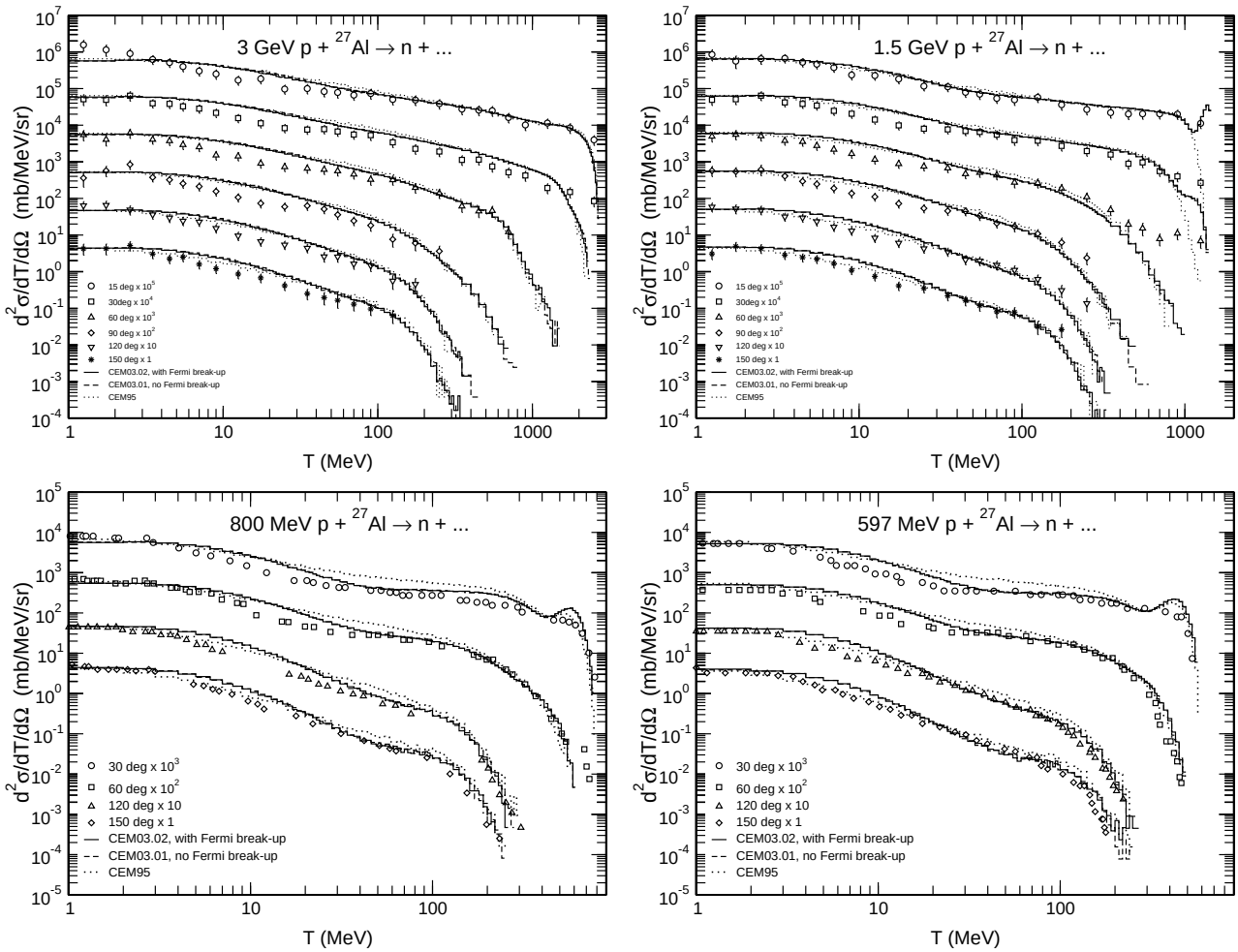

Figure 15: Experimental [20,31,32] double differential neutron spectra at 15, 30, 60, 90, 120, and 150 deg from 3.0, 1.5, 0.8, and 0.597 GeV p + Al (symbols) compared with results by CEM03.01 without considering the Fermi Break-up mode during the preequilibrium and evaporation stages of reactions (dashed histograms), with CEM03.02 that does consider the Fermi Break-up mode during the preequilibrium and evaporation stages of reactions (solid histograms), and with the old version of the code, CEM95 [8].

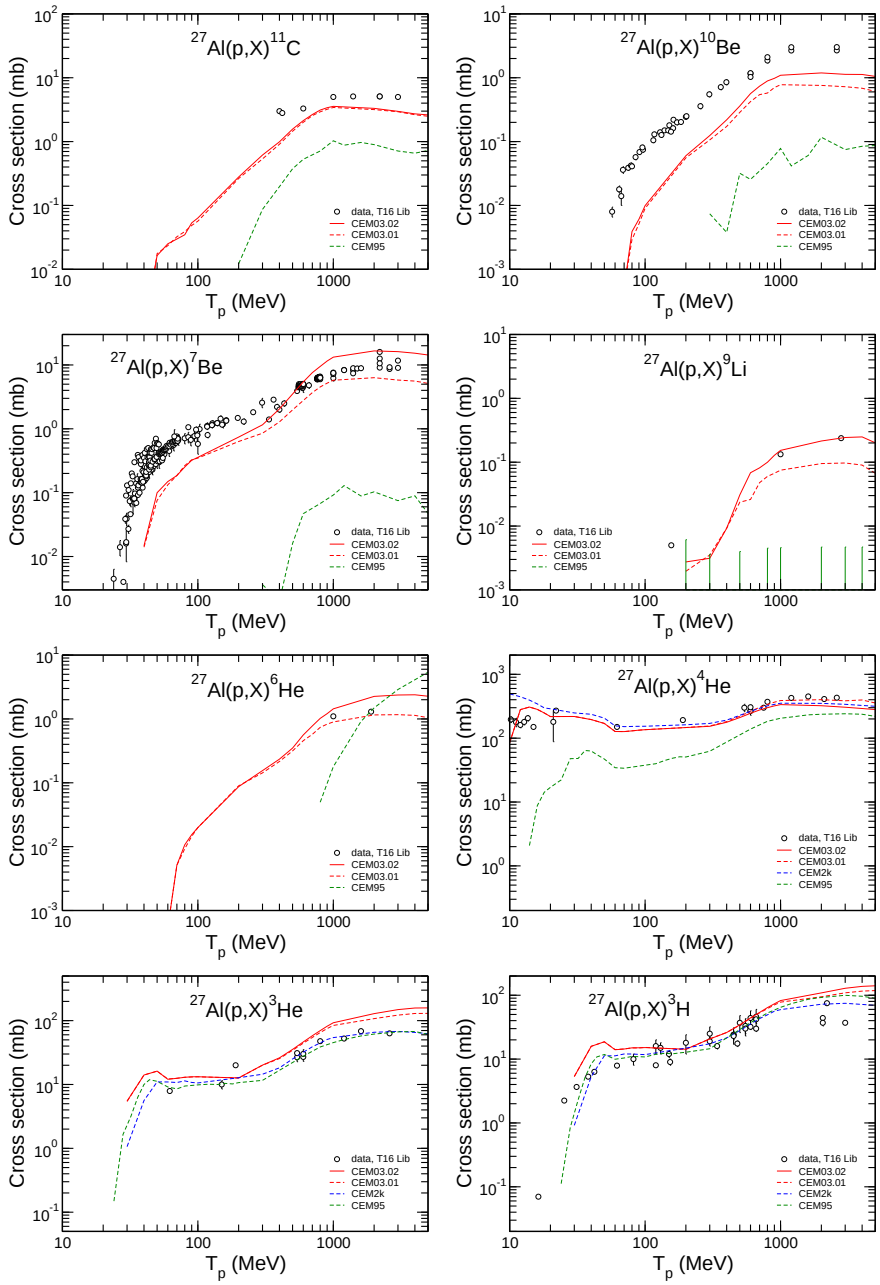

Figure 16: Excitation functions for the production of ^{11}C, ^{10}Be, ^{7}Be, ^{9}Li, ^{6}He, ^{4}He, ^{3}He, and ^{3}H from p+^{27}Al calculated with the CEM03.01 without considering the Fermi Break-up mode during the preequilibrium and evaporation stages of reactions (red dashed lines), with CEM03.02 that does consider this mode (red solid lines), with the old version of the Cascade-Exciton Model (CEM) realized in the code CEM95 available from NEA/OECD as the Code Package IAEA1247 [8] (green dashed lines), and with the improved 2000 version of CEM as realized in the code CEM2k [33] implemented into the transport code MCNPX 2.5.0 [34] (blue dashed lines). Experimental data (circles) are from the T-16 Lib compilation [30].

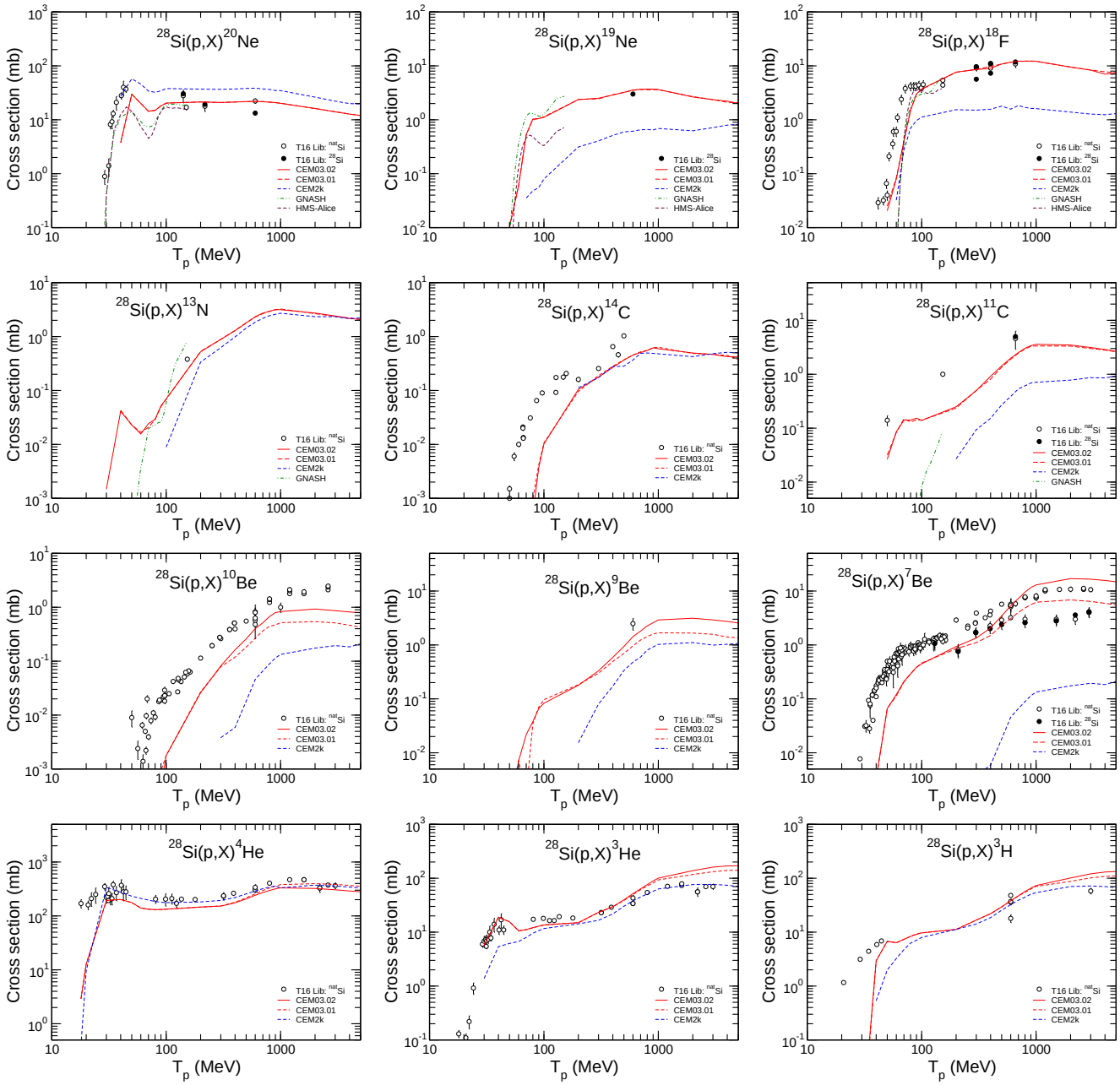

Figure 17: Excitation functions for the production of ^{20}Ne, ^{19}Ne, ^{18}F, ^{13}N, ^{14}C, ^{11}C, ^{10}Be, ^{9}Be, ^{7}Be, ^{4}He, ^{3}He, and ^{3}H from p+^{28}Si calculated with the CEM03.01 without considering the Fermi Break-up mode during the preequilibrium and evaporation stages of reactions (red dashed lines), with CEM03.02 that does consider this mode (red solid lines), with the improved 2000 version of CEM as realized in the code CEM2k [33] implemented into the transport code MCNPX 2.5.0 [34] (blue dashed lines), and with calculations by Mark Chadwick using the GNASH [35] (green dot-dashed lines) and HMS-Alice [36] (brown dashed lines) codes from Ref. [37]. Experimental data (circles) are from the T-16 Lib compilation [30].

After incorporation the updated CEM03.01 into MCNP6 and its verification and validation, the model was improved further to consider the Fermi Break-up mode of reactions during the preequilibrium and evaporation stages of reactions when $A < 13$, that allowed us to avoid production of some unstable residual nuclei that was allowed by previous versions of the model. This physically important feature is not considered yet by any other reaction simulation models. We call the latest version of our event generator considering this important feature as CEM03.02.

We suggest to consider in the future a possible permanent replacement in MCNP6 of the approximations by Barashenkov and Polanski used at present to describe the total reaction cross sections induced by nucleons, complex particles, and heavy ions with the NASA systematics by Tripathi, Cucinota, and Wilson, as an improved feature of MCNP6. Replacing the approximations by Barashenkov and Polanski for the total elastic cross sections used now in MCNP6 with the recently developed at NASA systematics would be also desirable, after a corresponding validation, verification, and testing against all available experimental data of both approximations.

REFERENCES

[1] X-5 Monte Carlo Team, "MCNP—A General Monte Carlo N-Particle Transport Code, Version 5. Volume I: Overview and Theory," LANL Report LA-UR-03-1987, Los Alamos (2003), RSICC Code Package CCC-730, http://www-rsicc.ornl.gov/rsiccnew/mcnp5-1.40release.htm

[2] Forrest B. Brown, "Monte Carlo Methods & MCNP Code Development," LANL Report LA-UR-05-2729, Los Alamos (2005); http://rsicc.ornl.gov/rsiccnew/MC2005_Presentations/Brown_PLENARY.pdf.

[3] Stepan G. Mashnik, Konstantin K. Gudima, Arnold J. Sierk, Mircea I. Baznat, and Nikolai V. Mokhov, "CEM03.01 User Manual," LANL Report LA-UR-05-7321, Los Alamos (2005); RSICC Code Package PSR-532; http://www-rsicc.ornl.gov/codes/psr/psr5/psr532.html.

[4] Konstantin K. Gudima, Stepan G. Mashnik, and Arnold J. Sierk, "User Manual for the code LAQGSM," LANL Report LA-UR-01-6804, Los Alamos (2001), http://lib-www.lanl.gov/la-pubs/00818645.pdf.

[5] S. G. Mashnik, K. K. Gudima, M. I. Baznat, A. J. Sierk, R. E. Prael, and N. V. Mokhov, "CEM03.01 and LAQGSM03.01 Versions of the Improved Cascade-Exciton Model (CEM) and Los Alamos Quark-Gluon String Model (LAQGSM) Codes," Research Note X-5-RN (U) 05-11; LANL Report LA-UR-05-2686, Los Alamos (2005).

[6] S. G. Mashnik, A. J. Sierk, K. K. Gudima, and M. I. Baznat, "CEM03 and LAQGSM03—New Modeling Tools for Nuclear Applications," *Journal of Physics: Conference Series*, **41**, 340 (2006).

[7] John S. Hendricks, Gregg W. McKinney, Holly R. Trellue, Joe W. Durkee, Joshua P. Finch, Michael L. Fensin, Michael R. James, Denise B. Pelowitz, Laurie S. Waters, Franz X. Gallmeier, Julian-Christophe David, "MCNPX, Version 2.6.B," Los Alamos National Laboratory Report LA-UR-06-3248 (June 1, 2006); mcnpx.lanl.gov/opendocs/versions/v26b/v26b.pdf.

[8] S. G. Mashnik, "User Manual for the code CEM95," Laboratory of Theoretical Physics, Joint Institute for Nuclear Research, Dubna, Russia; OECD Nuclear Energy Agency Data Bank, Le Seine Saint-Germain 12, Boulevard des Iles, F-92130 Issy-les-Moulineax, Paris, France, 1995; NEA/OECD Code Package IAEA1247, http://www.nea.fr/abs/html/iaea1247.html.

[9] S. G. Mashnik, A. J. Sierk, O. Bersillon, and T. Gabriel, "Cascade-Exciton Model Detailed Analysis of Proton Spallation at Energies from 10 MeV to 5 GeV," LANL Report LA-UR-97-2905, Los Alamos (1997); http://t2.lanl.gov/publications/publications.html.

[10] V. S. Barashenkov, *Cross Sections of Interaction of Particles and Nuclei with Nuclei*, (in Russian) JINR, Dubna (1993); see tabulated data at: http://www.nea.fr/html/dbdata/bara.html.

[11] E. M. Rimmer and P. S. Fisher, "Resonances in the (p,n) Reaction on ^{12}C," *Nucl. Phys. A*, **108**, 561 (1968).

[12] A. S. Iljinov, V. G. Semenov, M. P. Semenova, N. M. Sobolevsky, and L. V. Udovenko, "Production of Radionuclides at Intermediate Energies," Springer Verlag, Landolt-Börnstein, New Series, subvolumes **I/13a** (1991), **I/13b** (1992), **I/13c** (1993), and **I/13d** (1994).

[13] R. Bodemann, H.-J. Lange, I. Leya, R. Michel, T. Schienkel, R. Rösel, U. Herpers, H. J. Hofmann, B. Dittrich, M. Suter, W. Wölfli, B. Holmqvist, H. Condé, and P. Malmborg, "Production of Residual Nuclei by Proton-Induced Reactions on C, N, O, Mg, Al and Si," *Nucl. Instr. Meth. B*, **82**, 9 (1993).

[14] B. S. Amin, S. Biswas, D. Lal, and B. L. K. Somayajulu, "Radiochemical Measurements of ^{10}Be and ^{7}Be Formation Cross Sections in Oxygen by 135 and 550 MeV Protons," *Nucl. Phys. A*, **195**, 311 (1972).

[15] R. Michel, M. Gloris, H.-J. Lange, I. Leya, M. Lüpke, U. Herpers, B. Dittrich-Hannen, R. Rösel, Th. Schiekel, D. Filges, P. Dragovitsch, M. Suter, H.-J. Hofmann, W. Wölfli, P.-W. Kubik, H. Bauer, and R. Wieler, "Nuclide Production by Proton-Induced Reactions on Elements ($6 \leq Z \leq 29$) in the Energy Range from 800 to 2600 MeV," *Nucl. Instr. Meth. B*, **93**, 183 (1995).

[16] V. S. Barashenkov and V. D. Toneev, *Interaction of High Energy Particles and Nuclei with Atomic Nuclei*, (in Russian) Atomizdat, Moscow (1972).

[17] A. Yu. Konobeyev and Yu. A. Korovin, "Tritium Production in Materials from C to Bi Irradiated with Nucleons of Intermediate and High Energies," *Nucl. Instr. Meth. B*, **82**, 103 (1993).

[18] R. E. Prael, "Tally Edits for the MCNP6 GENXS Option," Research Note X-5-RN(U) 40-41, Los Alamos (2004).

[19] D. R. F. Cochran, P. N. Dean, P. A. M. Gram, E. A. Knapp, E. R. Martin, D. E. Nagle, R. B. Perkins, W. J. Shlaer, H. A. Thiessen, and E. D. Theriot, "Production of Charged Pions by 730-MeV Protons from Hydrogen and Selected Nuclei," *Phys. Rev. D*, **6**, 3085 (1972); LASL Report LA-5083-MS, Los Alamos (1972).

[20] K. Ishibashi, H. Takada, T. Nakomoto, N. Shigyo, K. Maehata, N. Matsufuji, S. Meigo, S. Chiba, M. Numajiri, Y. Watanabe, T. Nakamura, "Measurement of Neutron-Production Double-Differential Cross Sections for Nuclear Spallation Reaction Induced by 0.8, 1.5 and 3.0 GeV Protons", *J. Nucl. Sci. Techn.*, **34**, 529 (1997).

[21] T. Nakamoto, K. Ishibashi, N. Matsufuji, N. Shigyo, K. Maehata, H. Arima, S. Meigo, H. Takada, S. Chiba, and M. Numajiri, "Experimental Neutron-Production Double-Differential Cross Section for the Nuclear Reaction by 1.5 GeV π^+ Mesons Incident on Iron," *J. Nucl. Sci. Techn.*, **34**, 860 (1997).

[22] F. Rejmund, B. Mustapha, P. Armbruster, J. Benlliure, M. Bernas, A. Boudard, J. P. Dufour, T. Enqvist, R. Legrain, S. Leray, K.-H. Schmidt, C. Stéphan, J. Taieb, L. Tassan-Got, and C. Volant, "Measurement of Isotopic Cross Sections of Spallation Residues in 800 A MeV ^{197}Au + p Collisions," *Nucl. Phys. A*, **683**, 540 (2001); J. Benlliure, P. Armbruster, M. Bernas, A. Boudard, J. P. Dufour, T. Enqvist, R. Legrain, S. Leray, B. Mustapha, F. Rejmund, K.-H. Schmidt, C. Stéphan, L. Tassan-Got, and C. Volant, "Isotopic Production Cross Sections of Fission Residues in ^{197}Au-on-Proton Collisions at 800 A MeV," *Nucl. Phys. A*, **683**, 513 (2001).

[23] I. Dostrovsky, Z. Frankel, and G. Friedlander, "Monte Carlo Calculations of Nuclear Evaporation Processes. III. Application to Low-Energy Reactions," *Phys. Rev.*, **116**, 683 (1959).

[24] R. K. Tripathi, F. A. Cucinotta, and J. W. Wilson, "Accurate Universal Parameterization of Absorption Cross Sections," *Nucl. Instr. Meth. Phys. Res. B*, **117**, 347 (1996).

[25] C. Kalbach, "Towards a Global Exciton Model; Lessons at 14 MeV," *J. Phys. G: Nucl. Part. Phys.*, **24**, 847 (1998).

[26] H. H. K. Tang, G. R. Srinivasan, and N. Azziz, "Cascade Statistical Model for Nucleon-Induced Reactions on Light Nuclei in the Energy Range 50 MeV–1 GeV", *Phys. Rev. C*, **42**, 1598 (1990).

[27] V. S. Barashenkov and A. Polanski, "Electronic Guide for Nuclear Cross-Sections", Joint

Institute for Nuclear Research Communication JINR E2-94-417, Dubna, Russia (1994).

[28] A. Auce, R. F. Carlson, A. J. Cox, A. Ingemarsson, R. Johansson, P. U. Renberg, O. Sundberg, G. Tibell, and R. Zorro, "Reaction Cross Section for 75–190 MeV Alpha Particles on Targets from ^{12}C to ^{208}Pb," *Phys. Rev. C*, **50**, 871 (1994).

[29] L. V. Dubar, D. Sh. Eleukenov, L. I. Slyusarenko, and N. P. Yurkuts, "Parameterization of the Total Cross Sections of Reactions in the Intermediate Energy Region," *Yad. Fiz.* , **49**, 1239 (1989) [*Sov. J. Nucl. Phys.*, **49**, 771 (1989)].

[30] S. G. Mashnik, A. J. Sierk, K. A. Van Riper, and W. B. Wilson, "Prodiction and Validation of Isotope Production Cross Section Libraries for Neutrons and Protons to 1.7 GeV," LANL Report LA-UR-98-6000 (1998); Eprint: **nucl-th/9812071**; Proc. Forth Int. Workshop on Simulating Accelerator Radiation Environments (SARE-4), Hyatt Regency, Knoxville, TN, September 13-16, 1998 ORNL, 1999, pp. 151-162 (our T-16 Library "T-16 Lib" is updated permanently when new experimental data became available to us).

[31] W. B. Amian, R. C. Byrd, D. A. Clark, C. A. Goulding, M. M. Meier, G. L. Morgan,and C. E. Moss, "Differential Neutron Production Cross Sections for 597-MeV Protons," *Nucl. Sci. Eng.*, **115**, 1 (1993).

[32] W. B. Amian, R. C. Byrd, C. A. Goulding, M. M. Meier, G. L. Morgan, C. E. Moss, and D. A. Clark, "Differential Neutron Production Cross Sections for 800 MeV Protons," *Nucl. Sci. Eng.*, **112**, 78 (1992).

[33] S. G. Mashnik and A. J. Sierk, "CEM2k — Recent Developments in CEM," LANL Report LA-UR-00-5437, Los Alamos (2000); Proc. of the 2000 ANS/ENS Int. Meeting, Embedded Topical Meeting *Nuclear Applications of Accelerator Technology (AccApp00)*, November 12-16, 2000, Washington, DC (USA), American Nuclear Society, La Grange Park, IL, 2001, pp. 328-341; E-print: nucl-th/0011064; http://lib-www.lanl.gov/cgi-bin/getfile?00836384.pdf.

[34] John S. Hendricks, Gregg W. McKinney, Laurie S. Waters, Teresa L. Roberts, Harry W. Egdorf, Joshua P. Finch, Holly R. Trellue, Erick J. Pitcher, Douglas R. Mayo, Martyn T. Swinhoe, Stephen J. Tobin, Joe W. Durkee, Franz X. Gallmeier, Julian-Christophe David, and William B. Hamilton, and Julian Lebenhaft "MCNPX Extensions Version 2.5.0," LANL Report LA-UR-04-0570, Los Alamos (2004); http://mcnpx.lanl.gov/.

[35] P. G. Young, E. D. Arthur, and M. B. Chadwick, "Comprehensive Nuclear Model Calculations: Theory and Use of the GNASH Code," Proc. of the IAEA Workshop on Nuclear Reaction Data and Nuclear Reactors - Physics, Design, and Safety, Trieste, Italy, April 15 - May 17, 1996, edited by A. Gandini and G. Reffo (World Scientific Publishing, Ltd., Singapore, 1998), pp. 227-404.

[36] M. Blann, "New Precompound Decay Model," *Phys. Rev. C*, **54**, 1341 (1996); M. Blann and M. B. Chadwick, "New Precompound Decay Model: Angular Distributions," *Phys. Rev. C*,

57, 233 (1998).

[37] A. J. Koning, M. B. Chadwick, R. E. MacFarlane, S. G. Mashnik, and W. B. Wilson, "Neutron and Proton Transmutation-Activation Cross Section Libraries to 150 MeV for Application in Accelerator-Driven Systems and Radioactive Ion Beam Target-Design Studies," ECN Report ECN-R-98-012, Petten, The Netherlands (1998).

SGM:sgm

Distribution:
Eolus Team
R. B. Webster, X-3, F644
M. B. Chadwick, X-1, F699
L. A. McClellan, X-DO, B218
J. S. Sarracino, X-1-TA, F663
R. C. Little, X-1-NAD, F663
J. D. Zumbro, X-1-TA, F663
J. A. Carlson, T-16, B283
A. J. Sierk, T-16, B243
E. J. Pitcher, LANSCE-DO, H816
G. W. McKinney, X-3-MCC, K575
L. S. Waters, D-5, K575
J. S. Hendricks, X-3-MCC, K575
M. R. James, D-5, K575
X-DO file
X-3 file